

Inverse problem for a planar conductivity inclusion*

Doosung Choi^{†§} Johan Helsing[‡] Sangwoo Kang[§] Mikyoung Lim[§]

January 20, 2023

Abstract

This paper concerns the inverse problem of determining a planar conductivity inclusion. Our aim is to analytically recover from the generalized polarization tensors (GPTs), which can be obtained from exterior measurements, a homogeneous inclusion with arbitrary constant conductivity. The primary outcome of recovering a homogeneous inclusion is an inversion formula in terms of the GPTs for conformal mapping coefficients associated with the inclusion. To prove the formula, we establish matrix factorizations for the GPTs.

AMS subject classifications. 30C35, 35J05, 45P05

Keywords. Inverse conductivity problem; Lipschitz domain; Conformal mapping; Generalized polarization tensor

1 Introduction

The problem of determining electrical conductivity throughout a domain from boundary field measurements is of great interest which goes back many years [19, 20, 60, 61]. It has been extensively studied given its importance in real-life applications such as medical imaging and nondestructive testing. For instance, we refer to [18, 22, 30, 31, 52, 59] for the uniqueness results and to [3, 38, 43, 48, 49, 50, 53, 54, 55] for reconstruction methods. We also refer to [1, 17, 62] and the references therein for more results. Despite the theoretical and numerical results achieved, developing analytic inversion formulas is challenging because of the consequential nature of the nonlinearity and complexity of the inverse problem.

As building blocks for the detection problem of a conductivity inclusion, one can use the so-called generalized polarization tensors (GPTs), which are complex-valued matrices that generalize the polarization tensor (PT) [6, 56]. More precisely, the GPTs are the coefficients of the multipole expansion for the potential function that is perturbed due to the existence of the inclusion. They can be obtained from multistatic measurements [9], where a high signal-to-noise ratio is required for high-order terms [4]. Efficient algorithms have been developed to determine the location and

*This study was supported by National Research Foundation of Korea (NRF) grant funded by the Korean government (MSIT) (NRF-2021R1A2C1011804) and by the Swedish Research Council under contract 2021-03720.

[†]Department of Mathematics, Louisiana State University, Baton Rouge, LA 70808, USA.

[‡]Centre for Mathematical Sciences, Lund University, Box 118, 221 00 Lund, Sweden (johan.helsing@math.lth.se).

[§]Department of Mathematical Sciences, Korea Advanced Institute of Science and Technology, Daejeon 34141, Republic of Korea (7john@kaist.ac.kr, sangwoo.kang@kaist.ac.kr, mklim@kaist.ac.kr).

shape of inhomogeneities from the GPTs [14, 5, 6, 7, 15, 16, 24, 26] (see also [8] for the uniqueness result and [5, 25, 36] for other applications).

For the case of a planar simply connected inclusion, which is the focus of this paper, analytic shape recovery algorithms have been developed based on the complex analytical formulation for the conductivity transmission problem. The conformal mapping coefficients were explicitly expressed by the GPTs under the assumption that the inclusion is perfectly conducting or insulating [24, 26, 46]. However, only optimization approaches have been developed for an inclusion with general conductivity [12, 26]. The instances with arbitrary finite conductivity pose a specific complication because, unlike the inclusion with extreme conductivity, neither the Dirichlet nor the Neumann boundary condition is explicitly given in advance. It remains an interesting and open problem to generalize the inversion formula for the conformal mapping coefficients of an inclusion with extreme conductivity to the case of the inclusion with arbitrary finite conductivity. The objective of this paper is to provide a solution to this problem.

As the main tool, we use the concept of the Faber polynomial polarization tensors (FPTs), that is, the linear combinations of the GPTs with expansion coefficients defined by the Faber polynomials [25]. Indeed, for any simply connected domain in the complex plane, the Riemann mapping theorem assures the existence and uniqueness of the conformal mapping that transforms the exterior of a disk to the exterior of the domain. Then, this exterior conformal mapping generates the Faber polynomials, which form a basis for complex analytic functions in the domain. Recently, the FPTs were successfully applied to the asymptotic shape recovery of a conductivity inclusion [26] and the properties of the PT [23]. It is worth remarking that the layer potential operators associated with the domain admit matrix expressions with entries given by the Grunsky coefficients, which are expansion coefficients of the composition of the Faber polynomials and the exterior conformal mapping [44, 45].

As our main contribution, we propose a new factorization method for recovering a planar conductivity inclusion with arbitrary constant conductivity from the GPTs. For two semi-infinite matrices whose entries are scalar-valued complex contracted GPTs, we derive matrix factorization formulas in terms of the material parameter and conformal mapping coefficients associated with the inclusion. We rigorously prove that the formulas hold for either a smooth domain or a star-shaped domain with a Lipschitz boundary. Then, through the cancellation of the common factors in the two matrix factorizations, we derive an explicit inversion formula for the conformal mapping coefficients in terms of the GPTs and the conductivity value of the inclusion. We also obtain a fixed-point equation from which one can numerically compute the conductivity value. In conclusion, one can analytically recover the shape of an inclusion that possibly has a Lipschitz boundary after determining the conductivity value by a fixed-point computation. Our approach generalizes the shape recovery formulas for an inclusion with extreme conductivity obtained in [24, 26, 46] to an inclusion with arbitrary finite conductivity. Also, it significantly improves the asymptotic results of [7, 12, 13, 26] in that the resulting inversion formula of the shape recovery holds exactly rather than approximately.

We validate the proposed reconstruction approach with numerical experiments for inclusions of various shapes. To compute the GPTs, we solve a boundary integral equation involving the Neumann–Poincaré operator by using the Nyström discretization. For domains with corners in the numerical examples, we employ recursively compressed inverse preconditioning (RCIP) to compute the GPTs to a high degree of precision [42].

This paper is organized as follows. Section 2 describes the inverse problem of reconstructing a conductivity inclusion from exterior measurements and the concepts of the GPTs and FPTs.

Section 3 is devoted to reviewing shape recovery methods in the previous literature. In Section 4, we establish matrix factorizations for the GPTs and derive an inversion formula. In Section 5, we extend the proposed approach to a Lipschitz domain. We then validate our method with numerical examples in Section 6. We conclude with Section 7.

2 Preliminary

2.1 Problem formulation

Let Ω be a simply connected, bounded domain with a Lipschitz boundary in \mathbb{R}^2 . We assume that $\partial\Omega$ is a Jordan curve. We further assume that $\mathbb{R}^2 \setminus \overline{\Omega}$ and Ω have constant isotropic conductivities, respectively denoted by σ_m and σ_c , satisfying $0 < \sigma_c \neq \sigma_m < \infty$. Set $\lambda = \frac{\sigma_c + \sigma_m}{2(\sigma_c - \sigma_m)}$ if not specified otherwise. Note that $|\lambda| > \frac{1}{2}$. Consider the conductivity transmission problem:

$$\begin{cases} \Delta u = 0 & \text{in } \mathbb{R}^2 \setminus \partial\Omega, \\ u|^{+} = u|^{-} & \text{on } \partial\Omega, \\ \sigma_m \frac{\partial u}{\partial \nu}|^{+} = \sigma_c \frac{\partial u}{\partial \nu}|^{-} & \text{on } \partial\Omega, \\ (u - H)(x) = O(|x|^{-1}) & \text{as } |x| \rightarrow \infty, \end{cases} \quad (1)$$

where H is a given background potential that is entire harmonic. If there were no inclusion, the solution u would be H . The perturbation $u - H$ due to the inclusion depends on the geometry and material property of the inclusion and can be expressed in terms of layer potentials.

The Neumann–Poincaré (NP) operator for $\varphi \in L^2(\partial\Omega)$ is defined as

$$K_{\partial\Omega}^*[\varphi](x) = p.v. \frac{1}{2\pi} \int_{\partial\Omega} \frac{\langle x - y, \nu_x \rangle}{|x - y|^2} \varphi(y) d\sigma(y), \quad x \in \partial\Omega,$$

where *p.v.* stands for the Cauchy principal value and ν_x is the outward unit normal vector to $\partial\Omega$ at x . The operator $\lambda I - K_{\partial\Omega}^*$ is invertible on $L_0^2(\partial\Omega)$ (or $H_0^{-1/2}(\partial\Omega)$) for $|\lambda| \geq 1/2$ (see [34, 47, 63]).

The solution u admits the multipole expansion [9]: for $|x| > \sup\{|y| : y \in \Omega\}$,

$$(u - H)(x) = \sum_{|\alpha|, |\beta| \geq 1} \frac{(-1)^{|\beta|}}{\alpha! \beta!} \partial^\alpha H(0) M_{\alpha\beta}(\Omega, \lambda) \partial^\beta \Gamma(x) \quad (2)$$

with two-dimensional multi-indices α, β and the so-called generalized polarization tensors (GPTs)

$$M_{\alpha\beta}(\Omega, \lambda) = \int_{\partial\Omega} y^\beta (\lambda I - K_{\Omega}^*)^{-1} [\nu \cdot \nabla x^\alpha](y) d\sigma(y).$$

Here, $\Gamma(x)$ is the fundamental solution to the Laplacian, i.e., $\Gamma(x) = \frac{1}{2\pi} \ln|x|$. We refer the reader to [8] for the uniqueness of the inverse problem of determining the shape and conductivity value of an inclusion from the GPTs.

We identify $x = (x_1, x_2) \in \mathbb{R}^2$ with $z = x_1 + ix_2 \in \mathbb{C}$. We denote by $\Re\{\cdot\}$ and $\Im\{\cdot\}$ the real and imaginary parts of a complex number, respectively.

Definition 1 ([6]). Set $P_k(z) = z^k$ for each natural number k . For each $m, n = 1, 2, \dots$, we define the complex contracted generalized polarization tensors, which we also call the GPTs, as

$$\begin{aligned}\mathbb{N}_{mn}^{(1)}(\Omega, \lambda) &= \int_{\partial\Omega} P_n(z) (\lambda I - K_{\partial\Omega}^*)^{-1} \left[\frac{\partial P_m}{\partial \nu} \right] (z) d\sigma(z), \\ \mathbb{N}_{mn}^{(2)}(\Omega, \lambda) &= \int_{\partial\Omega} P_n(z) (\lambda I - K_{\partial\Omega}^*)^{-1} \left[\frac{\partial \overline{P_m}}{\partial \nu} \right] (z) d\sigma(z).\end{aligned}\tag{3}$$

We denote the semi-infinite matrices $\mathbb{N}^{(1)} = (\mathbb{N}_{mn}^{(1)})_{m,n=1}^\infty$ and $\mathbb{N}^{(2)} = (\mathbb{N}_{mn}^{(2)})_{m,n=1}^\infty$.

The GPTs, $\mathbb{N}_{mn}^{(1)}$ and $\mathbb{N}_{mn}^{(2)}$, are linear combinations of $M_{\alpha\beta}$, whose expansion coefficients are from the expansion of the complex polynomials into real polynomials. The values of the GPTs can be obtained from multistatic measurements [9].

In this paper, we consider the inverse problem of recovering the inclusion Ω and its conductivity σ_c (equivalently, $\lambda = \frac{\sigma_c + \sigma_m}{2(\sigma_c - \sigma_m)}$) from $\mathbb{N}_{mn}^{(1)}$ and $\mathbb{N}_{mn}^{(2)}$.

2.2 Faber polynomial polarization tensors (FPTs)

We remind the reader that Ω is a planar simply connected bounded domain. We now consider Ω as a domain in the complex plane \mathbb{C} . From the Riemann mapping theorem, there uniquely exist $\gamma > 0$ and a conformal mapping Ψ from $\{w \in \mathbb{C} : |w| > \gamma\}$ onto $\mathbb{C} \setminus \overline{\Omega}$ such that

$$\Psi(w) = w + a_0 + \frac{a_1}{w} + \frac{a_2}{w^2} + \dots.\tag{4}$$

One can numerically compute γ and a_n for a given domain Ω by solving a boundary integral equation [45, 64].

As a univalent function, Ψ defines the so-called Faber polynomials $\{F_m\}_{m=1}^\infty$ [35], which form a basis for complex analytic functions in Ω , by the relation

$$\frac{w\Psi'(w)}{\Psi(w) - z} = \sum_{m=0}^{\infty} \frac{F_m(z)}{w^m}, \quad z \in \overline{\Omega}, \quad |w| > \gamma.\tag{5}$$

The Faber polynomials F_m are monic polynomials of degree m that are uniquely determined by the conformal mapping coefficients $\{a_n\}_{0 \leq n \leq m-1}$ via the recursive relation (see, for instance, [32])

$$F_{m+1}(z) = zF_m(z) - ma_m - \sum_{n=0}^m a_n F_{m-n}(z), \quad m \geq 0.\tag{6}$$

In particular, we have

$$\begin{aligned}F_0(z) &= 1, \quad F_1(z) = z - a_0, \quad F_2(z) = z^2 - 2a_0z + a_0^2 - 2a_1, \\ F_3(z) &= z^3 - 3a_0z^2 + 3(a_0^2 - a_1)z - a_0^3 + 3a_0a_1 - 3a_2.\end{aligned}$$

Definition 2 ([25]). For each $m, n = 1, 2, \dots$, we define the Faber polynomial polarization tensors (FPTs) as

$$\begin{aligned}\mathbb{F}_{mn}^{(1)}(\Omega, \lambda) &= \int_{\partial\Omega} F_n(z) (\lambda I - K_{\partial\Omega}^*)^{-1} \left[\frac{\partial F_m}{\partial \nu} \right] (z) d\sigma(z), \\ \mathbb{F}_{mn}^{(2)}(\Omega, \lambda) &= \int_{\partial\Omega} F_n(z) (\lambda I - K_{\partial\Omega}^*)^{-1} \left[\frac{\partial \overline{F_m}}{\partial \nu} \right] (z) d\sigma(z).\end{aligned}$$

We denote the semi-infinite matrices $\mathbb{F}^{(1)} = (\mathbb{F}_{mn}^{(1)})_{m,n=1}^{\infty}$ and $\mathbb{F}^{(2)} = (\mathbb{F}_{mn}^{(2)})_{m,n=1}^{\infty}$.

We can express the Faber polynomial $F_m(z)$ as

$$F_m(z) = \sum_{n=0}^m p_{mn} z^n, \quad (7)$$

where for a fixed m , the coefficient p_{mn} depends only on $\{a_k\}_{0 \leq k \leq m-1}$. One can easily obtain recursive formulas for p_{mn} from (6). From (7) and the definition of the FPTs, it holds for each m, n that

$$\begin{aligned} \mathbb{F}_{mn}^{(1)} &= \sum_{k=1}^m \sum_{l=1}^n p_{mk} p_{nl} \mathbb{N}_{kl}^{(1)}, \\ \mathbb{F}_{mn}^{(2)} &= \sum_{k=1}^m \sum_{l=1}^n \overline{p_{mk}} p_{nl} \mathbb{N}_{kl}^{(2)}. \end{aligned} \quad (8)$$

2.3 Grunsky coefficients

An essential property of $F_m(z)$ is that $F_m(\Psi(w))$ has only one positive order term w^m . In other words,

$$F_m(\Psi(w)) = w^m + \sum_{n=1}^{\infty} c_{mn} w^{-n}, \quad |w| > \gamma,$$

where c_{mn} are the so-called Grunsky coefficients. It holds that (see [32])

$$nc_{mn} = mc_{nm} \quad \text{for all } m, n \in \mathbb{N} \quad (9)$$

and

$$\begin{aligned} c_{1m} &= a_m, \quad c_{m1} = ma_m, \\ c_{m(n+1)} &= c_{(m+1)n} - a_{m+n} + \sum_{s=1}^{m-1} a_{m-s} c_{sn} - \sum_{s=1}^{n-1} a_{n-s} c_{ms}, \quad m, n \geq 1. \end{aligned} \quad (10)$$

We can symmetrize the Grunsky coefficients as

$$g_{mn} = \sqrt{\frac{n}{m}} \frac{c_{mn}}{\gamma^{m+n}}. \quad (11)$$

From (9), it holds that

$$g_{mn} = g_{nm} \quad \text{for all } m, n \in \mathbb{N}. \quad (12)$$

We refer the reader to [32] for more details on the Faber polynomials and to [27, 28, 29, 33, 37, 51] for their applications in diverse areas.

We denote by C (resp., G) the semi-infinite matrix given by the Grunsky coefficients (resp., the symmetrized Grunsky coefficients), that is,

$$C = \begin{pmatrix} c_{11} & c_{12} & c_{13} & \cdots \\ c_{21} & c_{22} & c_{23} & \cdots \\ c_{31} & c_{32} & c_{33} & \cdots \\ \vdots & \vdots & \vdots & \ddots \end{pmatrix}, \quad G = \begin{pmatrix} g_{11} & g_{12} & g_{13} & \cdots \\ g_{21} & g_{22} & g_{23} & \cdots \\ g_{31} & g_{32} & g_{33} & \cdots \\ \vdots & \vdots & \vdots & \ddots \end{pmatrix}. \quad (13)$$

From (11), it holds that

$$G = \mathcal{N}^{-\frac{1}{2}} \gamma^{-\mathcal{N}} C \gamma^{-\mathcal{N}} \mathcal{N}^{\frac{1}{2}}, \quad (14)$$

where we set

$$\gamma^{\pm \mathcal{N}} = \begin{pmatrix} \gamma^{\pm 1} & 0 & 0 & \cdots \\ 0 & \gamma^{\pm 2} & 0 & \cdots \\ 0 & 0 & \gamma^{\pm 3} & \cdots \\ \vdots & \vdots & \vdots & \ddots \end{pmatrix}, \quad \mathcal{N}^{\pm \frac{1}{2}} = \begin{pmatrix} 1 & 0 & 0 & \cdots \\ 0 & \sqrt{2}^{\pm 1} & 0 & \cdots \\ 0 & 0 & \sqrt{3}^{\pm 1} & \cdots \\ \vdots & \vdots & \vdots & \ddots \end{pmatrix}. \quad (15)$$

Similarly to equation (15), the matrix $\gamma^{\pm 2\mathcal{N}}$ (resp., \mathcal{N} and \mathcal{N}^{-1}) denotes the diagonal matrix whose (n, n) -entries are $\gamma^{\pm 2n}$ (resp., n and n^{-1}).

3 Previous studies

We review previous studies on the shape recovery of a planar conductivity inclusion by using the concept of the GPTs. The first direction is to derive explicit expressions for the conformal mapping coefficients of the inclusion in terms of the GPTs, assuming that the inclusion has extreme conductivity, that is, the inclusion is either insulating or perfectly conducting (see Subsection 3.1). The second direction is to adopt an optimization approach for an inclusion with arbitrary constant conductivity (see Subsection 3.2).

3.1 Conformal mapping recovery for the extreme conductivity case

The exterior conformal mapping Ψ associated with Ω extends to the boundary of Ω as a homeomorphism by the Caratheodory extension theorem [21]. In particular, Ψ gives a natural parameterization for $\partial\Omega$ and, in particular, determines the shape of Ω .

For an inclusion with extreme conductivity, the multipole expansion of u admits an extension up to $\partial\Omega$ on which the Dirichlet or Neumann boundary condition is prescribed. For the case $\sigma_c = \infty$, u determines a holomorphic function $U(z)$ satisfying $u(x) = \Re\{U(z)\}$ and, thus,

$$\Re\{U(z)\} = \text{constant on } \partial\Omega.$$

For the case $\sigma_c = 0$, it holds that

$$\Im\{U(z)\} = \text{constant on } \partial\Omega. \quad (16)$$

Using this relation, the coefficients of Ψ were explicitly expressed by the GPTs for an inclusion with $\sigma_c = 0$ [24, 46]. Similar results could be derived for the perfectly conducting case by considering a harmonic conjugate of u .

The layer potential operators associated with Ω admit infinite series expansions with respect to basis functions defined with Ψ [45]. For an inclusion with a $C^{1,\alpha}$ boundary, one can then solve the conductivity inclusion problem by using these series expansions. As an application, we can express the FPTs with the Grunsky coefficients as follows.

Lemma 3.1 ([25]). *Let Ω have a $C^{1,\alpha}$ boundary. For each m, n , it holds that*

$$\begin{aligned}\mathbb{F}_{mn}^{(1)}(\Omega, \lambda) &= 4\pi n c_{mn} + 4\pi n (1 - 4\lambda^2) \left(C (4\lambda^2 I - \gamma^{-2N} \overline{C} \gamma^{-2N} C)^{-1} \right)_{mn}, \\ \mathbb{F}_{mn}^{(2)}(\Omega, \lambda) &= 8\pi n \lambda \gamma^{2m} \delta_{mn} + 8\pi n \lambda \gamma^{2m} (1 - 4\lambda^2) \left((4\lambda^2 I - \gamma^{-2N} \overline{C} \gamma^{-2N} C)^{-1} \right)_{mn}.\end{aligned}$$

Here, δ_{mn} is the Kronecker delta function.

For the case $\lambda = \pm \frac{1}{2}$, Lemma 3.1 implies that

$$\mathbb{F}_{m1}^{(1)}(\Omega, \lambda) = 4\pi c_{m1} \quad \text{for } m \geq 1, \quad (17)$$

$$\mathbb{F}_{11}^{(2)}(\Omega, \lambda) = 8\pi \lambda \gamma^2, \quad \mathbb{F}_{21}^{(2)}(\Omega, \lambda) = 0. \quad (18)$$

Using these relations and (10) for $n = 1$, one can completely recover the conformal mapping coefficients, where the expression formulas are much simpler than those derived in [24, 46] as follows.

Theorem 3.2 ([26]). *Let Ω be a simply connected, bounded $C^{1,\alpha}$ domain with $\sigma_c = 0$ or ∞ (equivalently, $\lambda = -\frac{1}{2}$ or $\frac{1}{2}$). The exterior conformal mapping Ψ associated with Ω (see (4)) satisfies*

$$\begin{aligned}\gamma^2 &= \frac{\lambda}{2\pi} \mathbb{N}_{11}^{(2)}(\Omega, \lambda), \quad a_0 = \frac{\mathbb{N}_{12}^{(2)}(\Omega, \lambda)}{2 \mathbb{N}_{11}^{(2)}(\Omega, \lambda)}, \\ a_m &= \frac{\lambda^2}{\pi m} \sum_{n=1}^m p_{mn} \mathbb{N}_{n1}^{(1)}(\Omega, \lambda), \quad m \geq 1,\end{aligned}$$

where $p_{m1}, p_{m2}, \dots, p_{mm}$ denote the coefficients of $F_m(z)$ of Ω as defined in (7). In particular, each a_m is uniquely determined by $\mathbb{N}_{12}^{(2)}$ and $\{\mathbb{N}_{n1}^{(1)}\}_{1 \leq n \leq m}$.

3.2 Optimization approach for the arbitrary conductivity case

Let D be an inclusion having the conductivity σ_c with a C^2 boundary given by a small perturbation of D_0 , that is,

$$\partial D = \{x + \varepsilon f(x) \nu_0(x) : x \in \partial D_0\} \quad (19)$$

with a real-valued function $f \in C^1(\partial D_0)$ and a small parameter $\varepsilon > 0$, where ν_0 is the outward unit normal vector to ∂D_0 . It then holds that (see [12])

$$\begin{aligned}& \sum_{\alpha, \beta} a_\alpha b_\beta M_{\alpha\beta}(D, \lambda) - \sum_{\alpha, \beta} a_\alpha b_\beta M_{\alpha\beta}(D_0, \lambda) \\ &= \varepsilon \left(\frac{\sigma_c}{\sigma_m} - 1 \right) \int_{\partial \Omega} f(x) \left[\frac{\partial v}{\partial \nu} \Big|^- \frac{\partial u}{\partial \nu} \Big|^- + \frac{\sigma_m}{\sigma_c} \frac{\partial v}{\partial T} \Big|^- \frac{\partial u}{\partial T} \Big|^- \right] (x) d\sigma(x) + O(\varepsilon^2),\end{aligned} \quad (20)$$

where u and v are the solutions to

$$\begin{cases} \Delta u = 0 & \text{in } D_0 \cup (\mathbb{R}^2 \setminus \overline{D_0}), \\ |u|^+ = |u|^- & \text{on } \partial D_0, \\ \sigma_m \frac{\partial u}{\partial \nu} \Big|^+ = \sigma_c \frac{\partial u}{\partial \nu} \Big|^- & \text{on } \partial D_0, \\ u(x) - H_1(x) = O(|x|^{-1}) & \text{as } |x| \rightarrow \infty \end{cases} \quad (21)$$

and

$$\begin{cases} \Delta v = 0 & \text{in } D_0 \cup (\mathbb{R}^2 \setminus \overline{D_0}), \\ \sigma_c v|^{+} = \sigma_m v|^{-} & \text{on } \partial D_0, \\ \frac{\partial v}{\partial \nu}|^{+} = \frac{\partial v}{\partial \nu}|^{-} & \text{on } \partial D_0, \\ v(x) - H_2(x) = O(|x|^{-1}) & \text{as } |x| \rightarrow \infty \end{cases} \quad (22)$$

with entire harmonic functions $H_1(x) = \sum_{\alpha} a_{\alpha} x^{\alpha}$ and $H_2(x) = \sum_{\beta} b_{\beta} x^{\beta}$.

Iterative methods have been developed for approximating the shape of an inclusion Ω by adopting an optimization approach, where the cost function for a test domain D has the form (with a fixed positive integer K) [7, 12]

$$J[D] = \frac{1}{2} \sum_{|\alpha|+|\beta| \leq K} \left| \sum_{\alpha, \beta} a_{\alpha} b_{\beta} M_{\alpha\beta}(D, \lambda) - \sum_{\alpha, \beta} a_{\alpha} b_{\beta} M_{\alpha\beta}(\Omega, \lambda) \right|^2.$$

Equation (20) provides the shape derivative for the cost function.

If D_0 is a disk, one can simply solve (21) and (22) and, by rewriting (20), derive asymptotic formulas for the Fourier coefficients of the shape perturbation function f as elementary functions of the GPTs (see [11]). By using the asymptotic formulas for f , one can non-iteratively approximate an inclusion Ω by considering it as a small perturbation of an equivalent disk, where we set D_0 as the equivalent ellipse and f as the perturbation from ∂D_0 to $\partial \Omega$.

If D_0 is an ellipse, the integral formula in (20) is too complicated in Cartesian coordinates to find an explicit analytic form. In [26], the curvilinear orthogonal coordinates and the Faber polynomials associated with the ellipse were successfully employed to derive explicit asymptotic formulas for the integral in (20). These asymptotic formulas (by taking D_0 as an equivalent ellipse) allow us to non-iteratively approximate an inclusion with arbitrary conductivity of general shape, including a straight or asymmetric shape (see [26] for the details).

4 Reconstruction of a smooth inclusion

For an inclusion with arbitrary constant conductivity, the boundary value of u in (1) is no longer explicit. Thus, it is a challenge to generalize Theorem 3.2 to the arbitrary constant conductivity case. In this section, we derive factorization formulas for two semi-infinite matrices whose entries are scalar-valued complex contracted GPTs and use the formulas to provide an answer to this problem as the primary conclusion of this paper.

4.1 Matrix factorizations for the GPTs

We denote by I the semi-infinite identity matrix. From (14), it holds that

$$4\lambda^2 I - \gamma^{-2\mathcal{N}} \overline{C} \gamma^{-2\mathcal{N}} C = \gamma^{-\mathcal{N}} \mathcal{N}^{\frac{1}{2}} (4\lambda^2 I - \overline{G}G) \gamma^{\mathcal{N}} \mathcal{N}^{-\frac{1}{2}}.$$

Lemma 3.1 and (14) lead to matrix factorizations for the FPTs.

Lemma 4.1. *Let Ω have a $C^{1,\alpha}$ boundary. The FPTs of Ω admit the matrix factorizations*

$$\begin{aligned} \mathbb{F}^{(1)} &= 4\pi \gamma^{\mathcal{N}} \mathcal{N}^{\frac{1}{2}} G \left[I + (1 - 4\lambda^2) (4\lambda^2 I - \overline{G}G)^{-1} \right] \mathcal{N}^{\frac{1}{2}} \gamma^{\mathcal{N}}, \\ \mathbb{F}^{(2)} &= 8\pi \lambda \gamma^{\mathcal{N}} \mathcal{N}^{\frac{1}{2}} \left[I + (1 - 4\lambda^2) (4\lambda^2 I - \overline{G}G)^{-1} \right] \mathcal{N}^{\frac{1}{2}} \gamma^{\mathcal{N}}. \end{aligned} \quad (23)$$

From the relations of the GPTs and FPTs, we can then obtain matrix factorizations for the GPTs. Set $P = (p_{mn})_{m,n=1}^{\infty}$ with p_{mn} given by (7). We can rewrite relations (8) in matrix form as

$$\begin{aligned}\mathbb{F}^{(1)} &= P \mathbb{N}^{(1)} P^T, \\ \mathbb{F}^{(2)} &= \overline{P} \mathbb{N}^{(2)} P^T,\end{aligned}\tag{24}$$

where \overline{P} and P^T denote the conjugate and transpose matrices of P , respectively. From (6), one can easily find that, for each $m \geq 1$,

$$p_{mm} = 1, \quad p_{(m+1)m} = -(m+1)a_0, \quad p_{mn} = 0 \quad \text{for all } n \geq m+1.\tag{25}$$

Indeed,

$$P = \begin{pmatrix} 1 & 0 & 0 & \cdots \\ -2a_0 & 1 & 0 & \cdots \\ 3a_0^2 - 3a_1 & -3a_0 & 1 & \cdots \\ \vdots & \vdots & \vdots & \ddots \end{pmatrix}.\tag{26}$$

Hence, P is lower triangular and invertible. Similarly, \overline{P} and P^T are invertible. From Lemma 4.1 and (24), we have the following theorem.

Theorem 4.2. *Let Ω have a $C^{1,\alpha}$ boundary. The GPTs of Ω admit the matrix factorizations*

$$\mathbb{N}^{(1)} = 4\pi P^{-1} \gamma^{\mathcal{N}} \mathcal{N}^{\frac{1}{2}} G \left[I + (1 - 4\lambda^2) (4\lambda^2 I - \overline{G}G)^{-1} \right] \mathcal{N}^{\frac{1}{2}} \gamma^{\mathcal{N}} (P^T)^{-1},\tag{27}$$

$$\mathbb{N}^{(2)} = 8\pi \lambda \overline{P}^{-1} \gamma^{\mathcal{N}} \mathcal{N}^{\frac{1}{2}} \left[I + (1 - 4\lambda^2) (4\lambda^2 I - \overline{G}G)^{-1} \right] \mathcal{N}^{\frac{1}{2}} \gamma^{\mathcal{N}} (P^T)^{-1}.\tag{28}$$

We note that the GPTs are expressed in terms of the exterior conformal mapping and the conductivity value of the inclusion. The matrix factorizations (27) and (28) have one common factor depending on λ , which satisfies

$$I + (1 - 4\lambda^2) (4\lambda^2 I - \overline{G}G)^{-1} = (I - \overline{G}G) (4\lambda^2 I - \overline{G}G)^{-1}.\tag{29}$$

In the instance that $\lambda = \pm \frac{1}{2}$ (that is, the insulating or perfectly conducting case), the common factor (29) is the identity matrix. It then follows the explicit expressions of the conformal mapping coefficients of Ω in Theorem 3.2. If $\lambda \neq \pm \frac{1}{2}$, it becomes more complicated to derive explicit formulas for the shape of the inclusion from (27) and (28).

4.2 Inversion formula

Our main idea to eliminate the common factor (29) between $\mathbb{N}^{(1)}$ and $\mathbb{N}^{(2)}$ is to consider

$$\mathbb{N}^{(1/2)} := \mathbb{N}^{(1)} (\mathbb{N}^{(2)})^{-1}.$$

We modify $\mathbb{N}^{(1)}$ and $\mathbb{N}^{(2)}$ as

$$\tilde{\mathbb{N}}^{(1)} = \mathbb{N}^{(1/2)} \mathbb{M} \mathbb{N}^{(2)}, \quad \tilde{\mathbb{N}}^{(2)} := \mathbb{M} \mathbb{N}^{(2)}\tag{30}$$

with

$$\mathbb{M} = \left(I - \overline{\mathbb{N}^{(1/2)}} \mathbb{N}^{(1/2)} \right) \left(I - 4\lambda^2 \overline{\mathbb{N}^{(1/2)}} \mathbb{N}^{(1/2)} \right)^{-1}.$$

Let $\tilde{\mathbb{N}}_{mn}^{(1)}$ and $\tilde{\mathbb{N}}_{mn}^{(2)}$ denote the (m, n) -component of $\tilde{\mathbb{N}}^{(1)}$ and $\tilde{\mathbb{N}}^{(2)}$, respectively. If $\lambda = \pm \frac{1}{2}$, then $\mathbb{M} = I$ and $\tilde{\mathbb{N}}^{(j)} = \mathbb{N}^{(j)}$, $j = 1, 2$. For $\tilde{\mathbb{N}}^{(2)}$, the same expression of $\mathbb{N}^{(2)}$ in (28) with extreme conductivity holds except the constant multiplication as follows.

Lemma 4.3. *For arbitrary constant σ_c satisfying $0 < \sigma_c \neq \sigma_m < \infty$, it holds that*

$$\tilde{\mathbb{N}}^{(2)} = \frac{2\pi}{\lambda} \overline{P}^{-1} \gamma^{2\mathcal{N}} \mathcal{N} (P^T)^{-1}.$$

Proof. By combining (27) and (28), we obtain

$$\mathbb{N}^{(1/2)} = (2\lambda)^{-1} P^{-1} \gamma^{\mathcal{N}} \mathcal{N}^{\frac{1}{2}} G \mathcal{N}^{-\frac{1}{2}} \gamma^{-\mathcal{N}} \overline{P} = (2\lambda)^{-1} P^{-1} C \gamma^{-2\mathcal{N}} \overline{P} \quad (31)$$

and, thus,

$$G = 2\lambda \mathcal{N}^{-\frac{1}{2}} \gamma^{-\mathcal{N}} P \mathbb{N}^{(1/2)} \overline{P}^{-1} \gamma^{\mathcal{N}} \mathcal{N}^{\frac{1}{2}}. \quad (32)$$

It then follows that

$$\overline{G}G = 4\lambda^2 \mathcal{N}^{-\frac{1}{2}} \gamma^{-\mathcal{N}} \overline{P} \overline{\mathbb{N}^{(1/2)}} \mathbb{N}^{(1/2)} \overline{P}^{-1} \gamma^{\mathcal{N}} \mathcal{N}^{\frac{1}{2}}. \quad (33)$$

Substituting (33) into (28) (also using (29)), we derive

$$\begin{aligned} \mathbb{N}^{(2)} &= 8\pi\lambda \overline{P}^{-1} \gamma^{\mathcal{N}} \mathcal{N}^{\frac{1}{2}} (I - \overline{G}G) (4\lambda^2 I - \overline{G}G)^{-1} \mathcal{N}^{\frac{1}{2}} \gamma^{\mathcal{N}} (P^T)^{-1} \\ &= \frac{2\pi}{\lambda} \left(I - 4\lambda^2 \overline{\mathbb{N}^{(1/2)}} \mathbb{N}^{(1/2)} \right) \left(I - \overline{\mathbb{N}^{(1/2)}} \mathbb{N}^{(1/2)} \right)^{-1} \overline{P}^{-1} \gamma^{2\mathcal{N}} (\mathcal{N}^{\frac{1}{2}})^2 (P^T)^{-1}. \end{aligned}$$

This completes the proof. \square

We now generalize the formula for the extreme conductivity case in Theorem 3.2 to the arbitrary conductivity case in terms of $\tilde{\mathbb{N}}^{(2)}$. If the GPTs of the inclusion are fully given, we can recover the exterior conformal mapping of the inclusion.

Theorem 4.4. *Let Ω be a simply connected, planar $C^{1,\alpha}$ domain with arbitrary constant conductivity σ_c satisfying $0 < \sigma_c \neq \sigma_m < \infty$ (that is, $\lambda = \frac{\sigma_c + \sigma_m}{2(\sigma_c - \sigma_m)}$ is an arbitrary real number satisfying $|\lambda| > \frac{1}{2}$). Let $\tilde{\mathbb{N}}^{(j)} = \tilde{\mathbb{N}}^{(j)}(\Omega, \lambda)$, $j = 1, 2$, be given by (30). Then,*

(a) λ satisfies the implicit equation

$$\lambda = \pi \frac{\tilde{\mathbb{N}}_{11}^{(2)} \tilde{\mathbb{N}}_{22}^{(2)} - \tilde{\mathbb{N}}_{12}^{(2)} \tilde{\mathbb{N}}_{21}^{(2)}}{\left(\tilde{\mathbb{N}}_{11}^{(2)} \right)^3}, \text{ and} \quad (34)$$

(b) the exterior conformal mapping coefficients associated with Ω satisfy the explicit formulas

$$\begin{aligned} \gamma^2 &= \frac{\lambda}{2\pi} \tilde{\mathbb{N}}_{11}^{(2)}(\Omega, \lambda), \quad a_0 = \frac{\tilde{\mathbb{N}}_{12}^{(2)}(\Omega, \lambda)}{2\tilde{\mathbb{N}}_{11}^{(2)}(\Omega, \lambda)}, \\ a_m &= \frac{\lambda^2}{\pi m} \sum_{n=1}^m p_{mn} \tilde{\mathbb{N}}_{n1}^{(1)}(\Omega, \lambda), \quad m \geq 1, \end{aligned} \quad (35)$$

where $p_{m1}, p_{m2}, \dots, p_{mm}$ denote the coefficients of $F_m(z)$ of Ω as defined in (7). In particular, each a_m is uniquely determined by λ , $\tilde{\mathbb{N}}_{12}^{(2)}$ and $\{\tilde{\mathbb{N}}_{n1}^{(1)}\}_{1 \leq n \leq m}$.

Proof. From Lemma 4.3, we have

$$\gamma^{2\mathcal{N}} = \frac{\lambda}{2\pi} \overline{P} \tilde{\mathbb{N}}^{(2)} P^T \mathcal{N}^{-1}. \quad (36)$$

From (25) and (36), we compute the $(1, 1)$ - and $(1, 2)$ -elements of $\gamma^{2\mathcal{N}}$:

$$\begin{aligned} \gamma^2 &= [\gamma^{2\mathcal{N}}]_{11} = \frac{\lambda}{2\pi} \tilde{\mathbb{N}}_{11}^{(2)}, \\ 0 &= [\gamma^{2\mathcal{N}}]_{12} = \frac{\lambda}{4\pi} [\overline{P} \tilde{\mathbb{N}}^{(2)} P^T]_{12} = \frac{\lambda}{4\pi} \tilde{\mathbb{N}}_{12}^{(2)} - \frac{\lambda}{2\pi} a_0 \tilde{\mathbb{N}}_{11}^{(2)}, \end{aligned} \quad (37)$$

and this implies that

$$a_0 = \frac{\tilde{\mathbb{N}}_{12}^{(2)}}{2\tilde{\mathbb{N}}_{11}^{(2)}}. \quad (38)$$

Let us continue to find a_m . We now substitute (36) into (31) and get

$$C = \frac{\lambda^2}{\pi} P \mathbb{N}^{(1/2)} \tilde{\mathbb{N}}^{(2)} P^T \mathcal{N}^{-1}.$$

From (10), we obtain

$$a_m = \frac{c_{m1}}{m} = \frac{\lambda^2}{\pi m} \sum_{n=1}^m p_{mn} [\mathbb{N}^{(1/2)} \tilde{\mathbb{N}}^{(2)}]_{n1} \quad \text{for each } m \geq 1.$$

For the constraint equation of λ , we compute the $(2, 2)$ -element of (36) by using (25), (37), and (38):

$$\begin{aligned} \frac{\lambda^2}{4\pi^2} (\tilde{\mathbb{N}}_{11}^{(2)})^2 &= [\gamma^{2\mathcal{N}}]_{22} \\ &= \frac{\lambda}{4\pi} [\overline{P} \tilde{\mathbb{N}}^{(2)} P^T]_{22} \\ &= \frac{\lambda}{4\pi} \left(4a_0 \overline{a_0} \tilde{\mathbb{N}}_{11}^{(2)} - 2a_0 \tilde{\mathbb{N}}_{21}^{(2)} - 2\overline{a_0} \tilde{\mathbb{N}}_{12}^{(2)} + \tilde{\mathbb{N}}_{22}^{(2)} \right) \\ &= \frac{\lambda}{4\pi} \left(\tilde{\mathbb{N}}_{22}^{(2)} - \frac{\tilde{\mathbb{N}}_{12}^{(2)}}{\tilde{\mathbb{N}}_{11}^{(2)}} \tilde{\mathbb{N}}_{21}^{(2)} \right). \end{aligned}$$

Since λ is nonzero, we finally get (34). \square

We note that the modified GPTs are defined by using λ as well as the GPTs. The right-hand side of (34) also depends on λ . We can numerically find the value of λ by an iterative algorithm as will be shown in Section 6. Then, the conformal radius γ and the coefficients a_m follow from $\tilde{\mathbb{N}}^{(1)}$, $\tilde{\mathbb{N}}^{(2)}$ and the computed value of λ .

Remark 1. According to Theorem 4.4, when the inclusion has finite conductivity, we need to know all the values of the GPTs to find a_m for a fixed m . However, if the conductivity is extreme, i.e., $\sigma_c = 0$ or ∞ , we only need the GPTs of finitely many indices as in Theorem 3.2.

5 Extension to a Lipschitz inclusion

We now generalize Theorems 4.2 and 4.4 to Lipschitz domains that satisfy the following shrinkable property with $s = a_0$.

Definition 3 (Star-shaped domain). *A set $D \subset \mathbb{R}^2$ is called a star-shaped domain with respect to a point $s_0 \in D$ if $\mu(D - s_0) + s_0 \Subset D$ for all $\mu \in [0, 1)$.*

For a closed Jordan curve Γ in \mathbb{C} , we say that Γ is smooth if it admits a parameterization $z(t) : [0, 2\pi) \rightarrow \mathbb{C}$ such that $z'(t)$ is continuous and $\neq 0$, following the definition in [58, Chapter 3.2]. A piecewise smooth Jordan curve without cusps is quasiconformal (refer to [2] and [58, Chapter 5.4] for the characterization of a quasiconformal curve). According to [57, Theorem 9.14], it holds that $\|G\|_{l^2 \rightarrow l^2} \leq \kappa$ for some $\kappa \in [0, 1)$ if and only if $\partial\Omega$ is quasiconformal. In particular, the matrix $4\lambda^2 I - \overline{G}G$ is invertible for all $|\lambda| \geq \frac{1}{2}$.

The following theorems are the main results in this section. We provide the proof of Theorem 5.1 at the end of Subsection 5.2.

Theorem 5.1 (Factorizations of the GPTs for a Lipschitz inclusion). *Let $\Omega \subset \mathbb{R}^2$ be a simply connected, bounded, and Lipschitz domain with arbitrary constant conductivity σ_c satisfying $0 < \sigma_c \neq \sigma_m < \infty$, where $\partial\Omega$ is a piecewise smooth Jordan curve without cusps. Assume that Ω is a star-shaped domain with respect to a_0 , where a_0 is the constant coefficient of the conformal mapping Ψ corresponding to Ω . Then the GPTs of Ω admit the matrix factorizations (27) and (28).*

In view of the derivation of (34) and (35), Theorem 5.1 directly leads to the following result for a Lipschitz inclusion.

Theorem 5.2. *Under the same assumptions for Ω as in Theorem 5.1, the shape recovery formulas (34) and (35) in Theorem 4.4 hold.*

5.1 Shape monotonicity of the GPTs

Harmonic combinations of the GPTs admit shape monotonicity:

Lemma 5.3 ([10]). *Let $\Omega' \subsetneq \Omega$ and J be a finite multi-index set. Let a_α be real-valued constant coefficients such that $h(x) = \sum_{\alpha \in J} a_\alpha x^\alpha$ is a harmonic polynomial. Then, we have*

$$\sum_{\alpha, \beta \in J} a_\alpha a_\beta M_{\alpha\beta}(\Omega, \lambda) > \sum_{\alpha, \beta \in J} a_\alpha a_\beta M_{\alpha\beta}(\Omega', \lambda) \quad \text{if } \lambda > \frac{1}{2}, \quad (39)$$

$$\sum_{\alpha, \beta \in J} a_\alpha a_\beta M_{\alpha\beta}(\Omega, \lambda) < \sum_{\alpha, \beta \in J} a_\alpha a_\beta M_{\alpha\beta}(\Omega', \lambda) \quad \text{if } \lambda < -\frac{1}{2}. \quad (40)$$

The following monotonicity property of the FPTs will be essentially used to prove Theorem 5.1 in Subsection 5.2.

Lemma 5.4. *The linear combinations of the FPTs*

$$\begin{aligned}
\mathbb{A}_{mn}^{(\pm 1)} &:= \operatorname{Re} \left\{ \mathbb{F}_{mm}^{(1)} + \mathbb{F}_{nn}^{(1)} + \mathbb{F}_{mm}^{(2)} + \mathbb{F}_{nn}^{(2)} \right\} \pm 2 \operatorname{Re} \left\{ \mathbb{F}_{mn}^{(1)} + \mathbb{F}_{mn}^{(2)} \right\}, \\
\mathbb{A}_{mn}^{(\pm 2)} &:= \operatorname{Re} \left\{ -\mathbb{F}_{mm}^{(1)} - \mathbb{F}_{nn}^{(1)} + \mathbb{F}_{mm}^{(2)} + \mathbb{F}_{nn}^{(2)} \right\} \mp 2 \operatorname{Re} \left\{ \mathbb{F}_{mn}^{(1)} - \mathbb{F}_{mn}^{(2)} \right\}, \\
\mathbb{A}_{mn}^{(\pm 3)} &:= \operatorname{Re} \left\{ \mathbb{F}_{mm}^{(1)} - \mathbb{F}_{nn}^{(1)} + \mathbb{F}_{mm}^{(2)} + \mathbb{F}_{nn}^{(2)} \right\} \mp 2 \operatorname{Im} \left\{ \mathbb{F}_{mn}^{(1)} + \mathbb{F}_{mn}^{(2)} \right\}, \\
\mathbb{A}_{mn}^{(\pm 4)} &:= \operatorname{Re} \left\{ -\mathbb{F}_{mm}^{(1)} + \mathbb{F}_{nn}^{(1)} + \mathbb{F}_{mm}^{(2)} + \mathbb{F}_{nn}^{(2)} \right\} \pm 2 \operatorname{Im} \left\{ \mathbb{F}_{mn}^{(1)} - \mathbb{F}_{mn}^{(2)} \right\}
\end{aligned} \tag{41}$$

have increasing and decreasing monotonicity with respect to the domain if $\lambda > \frac{1}{2}$ and $\lambda < -\frac{1}{2}$, respectively.

Proof. From the definition of the FPTs and the symmetry of the GPTs, we obtain

$$\begin{aligned}
&\operatorname{Re} \left\{ \mathbb{F}_{mm}^{(1)} + \mathbb{F}_{nn}^{(1)} + \mathbb{F}_{mm}^{(2)} + \mathbb{F}_{nn}^{(2)} \right\} \pm 2 \operatorname{Re} \left\{ \mathbb{F}_{mn}^{(1)} + \mathbb{F}_{mn}^{(2)} \right\} \\
&= 2 \int_{\partial\Omega} \operatorname{Re} \{F_m \pm F_n\} (\lambda I - K_{\partial\Omega}^*)^{-1} \left[\frac{\partial}{\partial\nu} \operatorname{Re} \{F_m \pm F_n\} \right] d\sigma.
\end{aligned}$$

From Lemma 5.3 with $h = \operatorname{Re}\{F_m \pm F_n\}$, we have the monotonicity for $\operatorname{Re}\{\mathbb{F}_{mm}^{(1)} + \mathbb{F}_{nn}^{(1)} + \mathbb{F}_{mm}^{(2)} + \mathbb{F}_{nn}^{(2)}\} \pm 2 \operatorname{Re}\{\mathbb{F}_{mn}^{(1)} + \mathbb{F}_{mn}^{(2)}\}$. Similarly, by applying Lemma 5.3 with $h = \operatorname{Im}\{F_m \pm F_n\}$, $\operatorname{Re}\{F_m \pm iF_n\}$, $\operatorname{Im}\{F_m \pm iF_n\}$, we complete the proof. \square

5.2 Proof of matrix factorizations for a Lipschitz inclusion

For $\epsilon > 0$, we define

$$\partial\Omega_\epsilon := \{\Psi(w) : |w| = \gamma_\epsilon\} \quad \text{with } \gamma_\epsilon = \gamma(1 + \epsilon),$$

where Ψ is given by (4). Since Ψ is conformal in $\{w : |w| > \gamma\}$, Ω_ϵ is an analytic domain and $\Omega \subset \Omega_\epsilon$. We now consider the scaled domain

$$\Omega^\delta := (1 - \delta)(\Omega - a_0) + a_0 \Subset \Omega \quad \text{for } \delta \in (0, 1), \tag{42}$$

where the subset relation holds due to the star-shaped condition for Ω . The exterior conformal mapping of Ω^δ is

$$\Psi^\delta(w) = w + a_0 + \frac{a_1^\delta}{w} + \frac{a_2^\delta}{w^2} + \dots \quad \text{for } |w| \geq \gamma^\delta \tag{43}$$

with $\gamma^\delta = (1 - \delta)\gamma$ and $a_n^\delta = (1 - \delta)^{n+1} a_n$. For any $\epsilon > 0$, we then set

$$\partial\Omega_\epsilon^\delta := \{\Psi^\delta(w) : |w| = \gamma_\epsilon^\delta\} \quad \text{with } \gamma_\epsilon^\delta = \gamma^\delta(1 + \epsilon). \tag{44}$$

Note that Ω_ϵ and Ω_ϵ^δ are simply connected analytic domains and that

$$\Omega_\epsilon^\delta = (\Omega^\delta)_\epsilon = (\Omega_\epsilon)^\delta.$$

For a fixed $\delta \in (0, 1)$, it follows from (42) that (see Figure 1)

$$\Omega_\epsilon^\delta \subsetneq \Omega \subsetneq \Omega_\epsilon \quad \text{for a sufficiently small } \epsilon > 0, \tag{45}$$

$$\Omega_\epsilon \downarrow \Omega \quad \text{and} \quad \Omega_\epsilon^\delta \downarrow \Omega^\delta \quad \text{as } \epsilon \rightarrow 0^+. \tag{46}$$

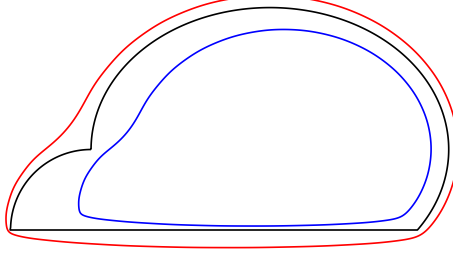


Figure 1: The blue, black, and red curves indicate $\partial\Omega_\epsilon^\delta$, $\partial\Omega$, and $\partial\Omega_\epsilon$ for a cap-shaped domain Ω , respectively, where Ω is a star-shaped domain with respect to a_0 .

Since Ω_ϵ is an analytic domain, (23) holds for Ω_ϵ , that is,

$$\begin{aligned}\mathbb{F}^{(1)}(\Omega_\epsilon, \lambda) &= 4\pi \gamma_\epsilon^\mathcal{N} \mathcal{N}^{\frac{1}{2}} G_\epsilon \left[I + (1 - 4\lambda^2) (4\lambda^2 I - \overline{G_\epsilon} G_\epsilon)^{-1} \right] \mathcal{N}^{\frac{1}{2}} \gamma_\epsilon^\mathcal{N}, \\ \mathbb{F}^{(2)}(\Omega_\epsilon, \lambda) &= 8\pi \lambda \gamma_\epsilon^\mathcal{N} \mathcal{N}^{\frac{1}{2}} \left[I + (1 - 4\lambda^2) (4\lambda^2 I - \overline{G_\epsilon} G_\epsilon)^{-1} \right] \mathcal{N}^{\frac{1}{2}} \gamma_\epsilon^\mathcal{N}.\end{aligned}\tag{47}$$

Here, G_ϵ is defined by (11) and (13) with γ replaced by γ_ϵ . In other words,

$$G_\epsilon = (1 + \epsilon)^{-\mathcal{N}} G (1 + \epsilon)^{-\mathcal{N}}.\tag{48}$$

One can easily find that rescaling and shifting of a domain do not change G . Namely,

$$G(\Omega^\delta) = G(\Omega).\tag{49}$$

Since $G(\Omega_\epsilon^\delta)$ is generated by the conformal mapping of Ω^δ with $\gamma_\epsilon^\delta = \gamma^\delta(1 + \epsilon)$ instead of γ^δ , one can easily find that

$$G(\Omega_\epsilon^\delta) = G(\Omega_\epsilon) = G_\epsilon.$$

Therefore, from (23), we have

$$\begin{aligned}\mathbb{F}^{(1)}(\Omega_\epsilon^\delta, \lambda) &= 4\pi (\gamma_\epsilon^\delta)^\mathcal{N} \mathcal{N}^{\frac{1}{2}} G_\epsilon \left[I + (1 - 4\lambda^2) (4\lambda^2 I - \overline{G_\epsilon} G_\epsilon)^{-1} \right] \mathcal{N}^{\frac{1}{2}} (\gamma_\epsilon^\delta)^\mathcal{N}, \\ \mathbb{F}^{(2)}(\Omega_\epsilon^\delta, \lambda) &= 8\pi \lambda (\gamma_\epsilon^\delta)^\mathcal{N} \mathcal{N}^{\frac{1}{2}} \left[I + (1 - 4\lambda^2) (4\lambda^2 I - \overline{G_\epsilon} G_\epsilon)^{-1} \right] \mathcal{N}^{\frac{1}{2}} (\gamma_\epsilon^\delta)^\mathcal{N},\end{aligned}\tag{50}$$

where the only difference from (47) and (50) is that $(\gamma_\epsilon^\delta)^\mathcal{N}$ is used instead of $\gamma_\epsilon^\mathcal{N}$.

From (47), (50) and the fact that $\gamma_\epsilon^\delta = (1 - \delta)\gamma_\epsilon$, the components of the FPTs of Ω_ϵ^δ converge to those of Ω_ϵ as $\delta \rightarrow 0^+$ when $\epsilon > 0$ is fixed. In other words, we have the following lemma.

Lemma 5.5. *For each fixed ϵ , we have*

$$\lim_{\delta \rightarrow 0^+} \mathbb{F}_{mn}^{(j)}(\Omega_\epsilon^\delta, \lambda) = \mathbb{F}_{mn}^{(j)}(\Omega_\epsilon, \lambda) \quad \text{for } j = 1, 2.\tag{51}$$

In the following, we investigate the convergence of $\mathbb{F}_{mn}^{(1)}(\Omega_\epsilon, \lambda)$ and $\mathbb{F}_{mn}^{(2)}(\Omega_\epsilon, \lambda)$ as ϵ goes to 0 (see Proposition 5.8). This is much more difficult to prove than Lemma 5.5. We start with a general property of a semi-infinite matrix.

Let $l^2(\mathbb{C})$ denote the vector space consisting of all complex sequences (x_m) satisfying $\sum_{m=1}^{\infty} |x_m|^2 < \infty$. We can interpret a semi-infinite matrix, namely $T = (t_{mn})$, as a linear operator from $l^2(\mathbb{C})$ to $l^2(\mathbb{C})$ given by

$$(x_m) \mapsto (y_m) \quad \text{with} \quad y_m = \sum_{n=1}^{\infty} t_{mn} x_n = \lim_{N \rightarrow \infty} \sum_{n=1}^N t_{mn} x_n, \quad (52)$$

assuming that the sequence of partial sums converges for each m and that $(y_m) \in l^2(\mathbb{C})$. We denote by $\|T\|$ the operator norm of T on $l^2(\mathbb{C})$, that is,

$$\|T\| = \|T\|_{l^2 \rightarrow l^2} = \sup_{\|x\|=1} \|Tx\|.$$

Assume that $\|T\| < \infty$. We put $x_n = \delta_{nk}$ to obtain

$$\|T\|^2 = \sup_{\|(x_n)\|=1} \sum_{m=1}^{\infty} \left| \sum_{n=1}^{\infty} t_{mn} x_n \right|^2 \geq \sum_{m=1}^{\infty} |t_{mk}|^2.$$

Let T^* denote the adjoint operator of T . Then, $T^* = (s_{mn})_{m,n=1}^{\infty}$ with $s_{mn} = t_{nm}$ and $\|T\| = \|T^*\|$. By applying the above inequality to T^* , we have

$$\sum_{m=1}^{\infty} |t_{mk}|^2 \leq \|T\|^2 \quad \text{and} \quad \sum_{m=1}^{\infty} |t_{km}|^2 \leq \|T\|^2 \quad \text{for each } k. \quad (53)$$

The Grunsky coefficients satisfy that (see, for instance, [32, Chapter 4.5])

$$\sum_{n=1}^{\infty} \left| \sum_{m=1}^{\infty} \sqrt{\frac{n}{m}} \frac{c_{mn}}{\gamma^{m+n}} x_m \right|^2 \leq \sum_{m=1}^{\infty} |x_m|^2 \quad (54)$$

for all complex sequences (x_m) . From (11) and the symmetry of G , we then have

$$\|G\|^2 = \sup_{\|(x_n)\|=1} \sum_{m=1}^{\infty} \left| \sum_{n=1}^{\infty} g_{mn} x_n \right|^2 = \sup_{\|(x_n)\|=1} \sum_{m=1}^{\infty} \left| \sum_{n=1}^{\infty} g_{nm} x_n \right|^2 \leq 1.$$

Assuming that $\partial\Omega$ is a piecewise smooth Jordan curve without cusps, we have (see [57, Theorem 9.14])

$$\|G\| \leq \kappa \quad \text{for some } \kappa < 1. \quad (55)$$

We now consider the operator G_ϵ (see (48)) as follows.

Lemma 5.6. *For all $\epsilon > 0$ and $|\lambda| \geq \frac{1}{2}$, we have*

$$\|G_\epsilon\| \leq \|G\|$$

and

$$\left\| (4\lambda^2 I - \overline{G}G)^{-1} \right\|, \left\| (4\lambda^2 I - \overline{G}_\epsilon G_\epsilon)^{-1} \right\| \leq \left(1 - \|G\|^2 \right)^{-1}.$$

Proof. From (48), it is straightforward to find that

$$\|G_\epsilon\| = \|(1 + \epsilon)^{-\mathcal{N}} G (1 + \epsilon)^{-\mathcal{N}}\| \leq \|(1 + \epsilon)^{-\mathcal{N}}\|^2 \|G\| \leq \|G\|. \quad (56)$$

From the assumption $|\lambda| \geq \frac{1}{2}$ and (56), we derive

$$\left\| (4\lambda^2 I - \overline{G}_\epsilon G_\epsilon)^{-1} \right\| \leq \frac{1}{4\lambda^2} \sum_{n=0}^{\infty} \left\| \frac{1}{4\lambda^2} \overline{G}_\epsilon G_\epsilon \right\|^n \leq \sum_{n=0}^{\infty} \|G_\epsilon\|^{2n} \leq (1 - \|G\|^2)^{-1}.$$

Similarly, we have boundedness for $(4\lambda^2 I - \overline{G}G)^{-1}$. \square

The following lemma is essential in proving the convergence of $\mathbb{F}_{mn}^{(1)}(\Omega_\epsilon, \lambda)$ and $\mathbb{F}_{mn}^{(2)}(\Omega_\epsilon, \lambda)$ as ϵ tends to zero.

Lemma 5.7. *Let $X = (x_{mn})_{m,n=1}^\infty$ and $Y = (y_{mn})_{m,n=1}^\infty$ be semi-infinite matrices depending on ϵ . Assume that X, Y are uniformly bounded with respect to ϵ , i.e., $\|X\|, \|Y\| \leq M < \infty$ for some constant M independent of ϵ . Then, the (m, n) -component of $X(G_\epsilon - G)Y$ satisfies that*

$$\lim_{\epsilon \rightarrow 0^+} [X(G_\epsilon - G)Y]_{mn} = 0 \quad \text{for each } m, n.$$

Proof. Fix $m, n \in \mathbb{N}$. We have

$$\begin{aligned} & \left| [X(G_\epsilon - G)Y]_{mn} \right| \\ &= \left| \sum_{k=1}^{\infty} \sum_{l=1}^{\infty} x_{mk} g_{kl} \left[(1 + \epsilon)^{-k-l} - 1 \right] y_{ln} \right| \\ &= \left| \sum_{k=1}^{\infty} \sum_{l=1}^{\infty} x_{mk} g_{kl} \left[\left((1 + \epsilon)^{-k} - 1 \right) (1 + \epsilon)^{-l} + \left((1 + \epsilon)^{-l} - 1 \right) \right] y_{ln} \right| \\ &\leq \sum_{k=1}^{\infty} \left| \left((1 + \epsilon)^{-k} - 1 \right) x_{mk} \sum_{l=1}^{\infty} g_{kl} (1 + \epsilon)^{-l} y_{ln} \right| + \sum_{k=1}^{\infty} \left| x_{mk} \sum_{l=1}^{\infty} g_{kl} \left((1 + \epsilon)^{-l} - 1 \right) y_{ln} \right| \\ &=: S_1 + S_2. \end{aligned}$$

It is sufficient to show that $S_1, S_2 \rightarrow 0$ as $\epsilon \rightarrow 0^+$.

From the Cauchy-Schwarz inequality and (54), we have

$$\begin{aligned} S_1 &\leq \left(\sum_{k=1}^{\infty} \left| \left((1 + \epsilon)^{-k} - 1 \right) x_{mk} \right|^2 \right)^{\frac{1}{2}} \left(\sum_{k=1}^{\infty} \left| \sum_{l=1}^{\infty} g_{kl} (1 + \epsilon)^{-l} y_{ln} \right|^2 \right)^{\frac{1}{2}} \\ &\leq \left(\sum_{k=1}^{\infty} (1 - (1 + \epsilon)^{-k})^2 |x_{mk}|^2 \right)^{\frac{1}{2}} \left(\sum_{l=1}^{\infty} |(1 + \epsilon)^{-l} y_{ln}|^2 \right)^{\frac{1}{2}}. \end{aligned} \quad (57)$$

It then follows from (53) that

$$\begin{aligned} \sum_{k=1}^{\infty} \left(1 - (1 + \epsilon)^{-k} \right)^2 |x_{mk}|^2 &\leq \sum_{k=1}^{\infty} |x_{mk}|^2 \leq \|X\|^2 \leq M^2, \\ \sum_{l=1}^{\infty} \left| (1 + \epsilon)^{-l} y_{ln} \right|^2 &\leq \sum_{l=1}^{\infty} |y_{ln}|^2 \leq \|Y\|^2 \leq M^2 \quad \text{independent of } \epsilon. \end{aligned}$$

Applying the dominated convergence theorem, we obtain

$$\lim_{\epsilon \rightarrow 0^+} \sum_{k=1}^{\infty} \left(1 - (1 + \epsilon)^{-k}\right)^2 |x_{mk}|^2 = \sum_{k=1}^{\infty} \lim_{\epsilon \rightarrow 0^+} \left(1 - (1 + \epsilon)^{-k}\right)^2 |x_{mk}|^2 = 0. \quad (58)$$

From (57) and (58), S_1 converges to 0 as $\epsilon \rightarrow 0^+$.

Similarly, we derive

$$\begin{aligned} S_2 &= \sum_{k=1}^{\infty} \left| x_{mk} \sum_{l=1}^{\infty} g_{kl} \left((1 + \epsilon)^{-l} - 1 \right) y_{ln} \right| \\ &\leq \left(\sum_{k=1}^{\infty} |x_{mk}|^2 \right)^{\frac{1}{2}} \left(\sum_{k=1}^{\infty} \left| \sum_{l=1}^{\infty} g_{kl} \left((1 + \epsilon)^{-l} - 1 \right) y_{ln} \right|^2 \right)^{\frac{1}{2}} \\ &\leq \|X\| \left(\sum_{l=1}^{\infty} \left(1 - (1 + \epsilon)^{-l}\right)^2 |y_{ln}|^2 \right)^{\frac{1}{2}} \rightarrow 0 \quad \text{as } \epsilon \rightarrow 0^+. \end{aligned} \quad (59)$$

This completes the proof. \square

Proposition 5.8. *As ϵ tends to zero, the right-hand sides of (47) converge to the formulas with γ in the place of γ_ϵ , that is, for each m, n ,*

$$\begin{aligned} \lim_{\epsilon \rightarrow 0^+} \mathbb{F}_{mn}^{(1)}(\Omega_\epsilon, \lambda) &= \left[4\pi \gamma^\mathcal{N} \mathcal{N}^{\frac{1}{2}} G \left[I + (1 - 4\lambda^2) (4\lambda^2 I - \overline{G}G)^{-1} \right] \mathcal{N}^{\frac{1}{2}} \gamma^\mathcal{N} \right]_{mn}, \\ \lim_{\epsilon \rightarrow 0^+} \mathbb{F}_{mn}^{(2)}(\Omega_\epsilon, \lambda) &= \left[8\pi \lambda \gamma^\mathcal{N} \mathcal{N}^{\frac{1}{2}} \left[I + (1 - 4\lambda^2) (4\lambda^2 I - \overline{G}G)^{-1} \right] \mathcal{N}^{\frac{1}{2}} \gamma^\mathcal{N} \right]_{mn}. \end{aligned} \quad (60)$$

Proof. Since $\gamma_\epsilon^\mathcal{N} \mathcal{N}^{\frac{1}{2}} G_\epsilon \mathcal{N}^{\frac{1}{2}} \gamma_\epsilon^\mathcal{N} = C = \gamma^\mathcal{N} \mathcal{N}^{\frac{1}{2}} G \mathcal{N}^{\frac{1}{2}} \gamma^\mathcal{N}$, we cancel out the first term of $\mathbb{F}_{mn}^{(1)}$ and get

$$\begin{aligned} &\mathbb{F}_{mn}^{(1)}(\Omega_\epsilon, \lambda) - \left[4\pi \gamma^\mathcal{N} \mathcal{N}^{\frac{1}{2}} G \left[I + (1 - 4\lambda^2) (4\lambda^2 I - \overline{G}G)^{-1} \right] \mathcal{N}^{\frac{1}{2}} \gamma^\mathcal{N} \right]_{mn} \\ &= 4\pi \sqrt{mn} (1 - 4\lambda^2) \left(\gamma_\epsilon^{m+n} \left[G_\epsilon (4\lambda^2 I - \overline{G}_\epsilon G_\epsilon)^{-1} \right]_{mn} - \gamma^{m+n} \left[G (4\lambda^2 I - \overline{G}G)^{-1} \right]_{mn} \right). \end{aligned}$$

We then have

$$\begin{aligned} &\gamma_\epsilon^{m+n} \left[G_\epsilon (4\lambda^2 I - \overline{G}_\epsilon G_\epsilon)^{-1} \right]_{mn} - \gamma^{m+n} \left[G (4\lambda^2 I - \overline{G}G)^{-1} \right]_{mn} \\ &= \gamma_\epsilon^{m+n} \left[(G_\epsilon - G) (4\lambda^2 I - \overline{G}_\epsilon G_\epsilon)^{-1} \right]_{mn} \\ &\quad + \gamma_\epsilon^{m+n} \left[G (4\lambda^2 I - \overline{G}_\epsilon G_\epsilon)^{-1} (\overline{G}_\epsilon - \overline{G}) G_\epsilon (4\lambda^2 I - \overline{G}G)^{-1} \right]_{mn} \\ &\quad + \gamma_\epsilon^{m+n} \left[G (4\lambda^2 I - \overline{G}_\epsilon G_\epsilon)^{-1} \overline{G} (G_\epsilon - G) (4\lambda^2 I - \overline{G}G)^{-1} \right]_{mn} \\ &\quad + (\gamma_\epsilon^{m+n} - \gamma^{m+n}) \left[G (4\lambda^2 I - \overline{G}G)^{-1} \right]_{mn}. \end{aligned}$$

From Lemma 5.6 and Lemma 5.7, this term converges to 0 as $\epsilon \rightarrow 0^+$.

Similarly, it holds that

$$\begin{aligned}
& \mathbb{F}_{mn}^{(2)}(\Omega_\epsilon, \lambda) - \left[8\pi\lambda \gamma^\mathcal{N} \mathcal{N}^{\frac{1}{2}} \left[I + (1 - 4\lambda^2) (4\lambda^2 I - \overline{G}G)^{-1} \right] \mathcal{N}^{\frac{1}{2}} \gamma^\mathcal{N} \right]_{mn} \\
&= 8\pi\lambda\sqrt{mn} \left(\gamma_\epsilon^{m+n} - \gamma^{m+n} \right) \\
&+ 8\pi\lambda\sqrt{mn} (1 - 4\lambda^2) \left(\gamma_\epsilon^{m+n} \left[(4\lambda^2 I - \overline{G}_\epsilon G_\epsilon)^{-1} \right]_{mn} - \gamma^{m+n} \left[(4\lambda^2 I - \overline{G}G)^{-1} \right]_{mn} \right).
\end{aligned}$$

The first term converges to 0 as $\epsilon \rightarrow 0^+$. The second terms satisfies

$$\begin{aligned}
& \gamma_\epsilon^{m+n} \left[(4\lambda^2 I - \overline{G}_\epsilon G_\epsilon)^{-1} \right]_{mn} - \gamma^{m+n} \left[(4\lambda^2 I - \overline{G}G)^{-1} \right]_{mn} \\
&= (\gamma_\epsilon^{m+n} - \gamma^{m+n}) \left[(4\lambda^2 I - \overline{G}G)^{-1} \right]_{mn} \\
&+ \gamma_\epsilon^{m+n} \left[(4\lambda^2 I - \overline{G}_\epsilon G_\epsilon)^{-1} \overline{G}_\epsilon (G_\epsilon - G) (4\lambda^2 I - \overline{G}G)^{-1} \right]_{mn} \\
&+ \gamma_\epsilon^{m+n} \left[(4\lambda^2 I - \overline{G}_\epsilon G_\epsilon)^{-1} (\overline{G}_\epsilon - \overline{G}) G (4\lambda^2 I - \overline{G}G)^{-1} \right]_{mn}.
\end{aligned}$$

From Lemma 5.6 and Lemma 5.7, this term converges to 0 as $\epsilon \rightarrow 0^+$. Hence, we prove the proposition. \square

Let $\delta \in (0, 1)$ be fixed. By applying Proposition 5.8 to Ω_ϵ^δ and using (49), we have

$$\begin{aligned}
\lim_{\epsilon \rightarrow 0^+} \mathbb{F}_{mn}^{(1)}(\Omega_\epsilon^\delta, \lambda) &= \left[4\pi (\gamma^\delta)^\mathcal{N} \mathcal{N}^{\frac{1}{2}} G \left[I + (1 - 4\lambda^2) (4\lambda^2 I - \overline{G}G)^{-1} \right] \mathcal{N}^{\frac{1}{2}} (\gamma^\delta)^\mathcal{N} \right]_{mn}, \\
\lim_{\epsilon \rightarrow 0^+} \mathbb{F}_{mn}^{(2)}(\Omega_\epsilon^\delta, \lambda) &= \left[8\pi\lambda (\gamma^\delta)^\mathcal{N} \mathcal{N}^{\frac{1}{2}} \left[I + (1 - 4\lambda^2) (4\lambda^2 I - \overline{G}G)^{-1} \right] \mathcal{N}^{\frac{1}{2}} (\gamma^\delta)^\mathcal{N} \right]_{mn}.
\end{aligned}$$

Because of $\gamma^\delta = (1 - \delta)\gamma$, one can easily find that $\lim_{\epsilon \rightarrow 0^+} \mathbb{F}_{mn}^{(j)}(\Omega_\epsilon^\delta, \lambda)$ converges to the right-hand sides of the equations in (60) as $\delta \rightarrow 0^+$. In view of Lemma 5.5 and Proposition 5.8, we conclude that

$$\lim_{\epsilon \rightarrow 0^+} \lim_{\delta \rightarrow 0^+} \mathbb{F}_{mn}^{(j)}(\Omega_\epsilon^\delta, \lambda) = \lim_{\epsilon \rightarrow 0^+} \mathbb{F}_{mn}^{(j)}(\Omega_\epsilon, \lambda) = \lim_{\delta \rightarrow 0^+} \lim_{\epsilon \rightarrow 0^+} \mathbb{F}_{mn}^{(j)}(\Omega_\epsilon^\delta, \lambda) \quad \text{for } j = 1, 2. \quad (61)$$

Proof of Theorem 5.1. From (24) and the fact that P is invertible, it is sufficient to prove that the FPTs of Ω satisfy (23) under the same assumptions as in Theorem 5.1.

Fix indices m, n . Assume that $\lambda > \frac{1}{2}$. As in Lemma 5.4, we set

$$\mathbb{A}_{mn}^{(+1)} = \text{Re} \left\{ \mathbb{F}_{mm}^{(1)} + \mathbb{F}_{nn}^{(1)} + \mathbb{F}_{mm}^{(2)} + \mathbb{F}_{nn}^{(2)} \right\} + 2\text{Re} \left\{ \mathbb{F}_{mn}^{(1)} + \mathbb{F}_{mn}^{(2)} \right\}.$$

From (61), it holds that

$$\lim_{\epsilon \rightarrow 0^+} \mathbb{A}_{mn}^{(1)}(\Omega_\epsilon, \lambda) = \lim_{\delta \rightarrow 0^+} \lim_{\epsilon \rightarrow 0^+} \mathbb{A}_{mn}^{(1)}(\Omega_\epsilon^\delta, \lambda). \quad (62)$$

From Lemma 5.4 and the fact that $\Omega \subsetneq \Omega_\epsilon$ for $\epsilon > 0$, we have

$$\lim_{\epsilon \rightarrow 0^+} \mathbb{A}_{mn}^{(1)}(\Omega_\epsilon, \lambda) \geq \mathbb{A}_{mn}^{(1)}(\Omega, \lambda) \quad (63)$$

On the other hand, (45) and the monotonicity of $\mathbb{A}_{mn}^{(1)}$ imply that

$$\lim_{\epsilon \rightarrow 0^+} \mathbb{A}_{mn}^{(1)}(\Omega_\epsilon^\delta, \lambda) \leq \mathbb{A}_{mn}^{(1)}(\Omega, \lambda) \quad \text{for each fixed } \delta \in (0, 1).$$

Therefore, we derive

$$\lim_{\delta \rightarrow 0^+} \lim_{\epsilon \rightarrow 0^+} \mathbb{A}_{mn}^{(1)}(\Omega_\epsilon^\delta, \lambda) \leq \mathbb{A}_{mn}^{(1)}(\Omega, \lambda).$$

By applying this relation to (62) and (63), we conclude that

$$\mathbb{A}_{mn}^{(1)}(\Omega, \lambda) = \lim_{\epsilon \rightarrow 0^+} \mathbb{A}_{mn}^{(1)}(\Omega_\epsilon, \lambda).$$

One can also prove this relation for $\lambda < -\frac{1}{2}$.

Furthermore, similar relations hold for $\mathbb{A}_{mn}^{(-1)}$ and $\mathbb{A}_{mn}^{(\pm j)}$, $j = 2, 3, 4$. Note that $\mathbb{F}_{nm}^{(1)}$ and $\mathbb{F}_{nm}^{(2)}$ are linear combinations of $\mathbb{A}_{mn}^{(\pm j)}$, $j = 1, 2, 3, 4$. It then directly follows that, for each m, n ,

$$\mathbb{F}_{mn}^{(k)}(\Omega, \lambda) = \lim_{\epsilon \rightarrow 0^+} \mathbb{F}_{mn}^{(k)}(\Omega_\epsilon, \lambda), \quad k = 1, 2.$$

Combining this convergence and Proposition 5.8, we conclude that the factorization (23) also holds for Ω that satisfies the assumptions in Theorem 5.1. \square

6 Numerical results

In this section, we propose a semi-analytic imaging scheme for a planar conductivity inclusion with arbitrary constant conductivity based on Theorems 4.4 and 5.2. To demonstrate the validity of the proposed reconstruction approach, we present numerical simulations with objects of different shapes.

6.1 Reconstruction scheme

Let Ω be an unknown inclusion having constant conductivity σ_c . Set $\lambda = \frac{\sigma_c + \sigma_m}{2(\sigma_c - \sigma_m)}$. For an inclusion with a $C^{1,\alpha}$ boundary, we apply Theorem 4.4 with measurements of $\mathbb{N}^{(1)}$ and $\mathbb{N}^{(2)}$. By Theorem 5.2, the same reconstruction procedure is valid for inclusions with corners.

We first find λ by using the constraint equation (34) in Theorem 4.4 (a), that is,

$$\lambda = \pi \frac{\tilde{\mathbb{N}}_{11}^{(2)} \tilde{\mathbb{N}}_{22}^{(2)} - \tilde{\mathbb{N}}_{12}^{(2)} \tilde{\mathbb{N}}_{21}^{(2)}}{\left(\tilde{\mathbb{N}}_{11}^{(2)}\right)^3}. \quad (64)$$

We note that the modified GPTs $\tilde{\mathbb{N}}^{(1)}(\Omega, \lambda)$ and $\tilde{\mathbb{N}}^{(2)}(\Omega, \lambda)$ are defined by (30) in terms of λ and the original contracted GPTs $\mathbb{N}^{(1)}(\Omega, \lambda)$ and $\mathbb{N}^{(2)}(\Omega, \lambda)$. We can rewrite (64) as

$$\lambda = f(\lambda), \quad f(t) := \pi \frac{\tilde{\mathbb{N}}_{11}^{(2)}(t) \tilde{\mathbb{N}}_{22}^{(2)}(t) - \tilde{\mathbb{N}}_{12}^{(2)}(t) \tilde{\mathbb{N}}_{21}^{(2)}(t)}{\left(\tilde{\mathbb{N}}_{11}^{(2)}(t)\right)^3}$$

with a variable $t \in (-1/2, 1/2)$ and

$$\begin{aligned}\tilde{\mathbb{N}}^{(1)}(t) &:= \mathbb{N}^{(1/2)} \mathbb{M}(t) \mathbb{N}^{(2)}, \quad \tilde{\mathbb{N}}^{(2)}(t) := \mathbb{M}(t) \mathbb{N}^{(2)}, \\ \mathbb{M}(t) &= \left(I - \overline{\mathbb{N}^{(1/2)}} \mathbb{N}^{(1/2)} \right) \left(I - 4t^2 \overline{\mathbb{N}^{(1/2)}} \mathbb{N}^{(1/2)} \right)^{-1},\end{aligned}$$

where $\mathbb{N}^{(1)} = \mathbb{N}^{(1)}(\Omega, \lambda)$, $\mathbb{N}^{(2)} = \mathbb{N}^{(2)}(\Omega, \lambda)$ and $\mathbb{N}^{(1/2)} = \mathbb{N}^{(1)}(\mathbb{N}^{(2)})^{-1}$ are given by measurements and are not modified by t . Since it is not possible to explicitly solve (64) for λ , we instead apply the fixed-point iteration method to find the numerical solution. Afterward, we retrieve the conformal mapping coefficients γ , a_0 , and a_m by the explicit formula (35) in Theorem 4.4 (b).

To develop the recovery method to be more realistic, we replace the semi-infinite matrices of the contacted GPTs by their finite section matrices. In other words, for some $\text{Ord} \geq 2$, we approximate $\mathbb{N}^{(1)}$, $\mathbb{N}^{(2)}$ by the truncated matrices as

$$\mathbb{N}^{(j)} \approx \left(\mathbb{N}_{mn}^{(j)} \right)_{1 \leq m, n \leq \text{Ord}}, \quad j = 1, 2, \quad (65)$$

and compute $\mathbb{N}^{(1/2)} = \mathbb{N}^{(1)}(\mathbb{N}^{(2)})^{-1}$ with the truncated matrices. With these finite approximations of $\mathbb{N}^{(1)}$, $\mathbb{N}^{(2)}$ and $\mathbb{N}^{(1/2)}$, we recover the conductivity constant σ_c (or, λ) and the shape of Ω by the following two-step procedure.

- **Step 1.** Set the initial guess as

$$\lambda_0 = \pi \frac{\mathbb{N}_{11}^{(2)}(\Omega, \lambda) \mathbb{N}_{22}^{(2)}(\Omega, \lambda) - \mathbb{N}_{12}^{(2)}(\Omega, \lambda) \mathbb{N}_{21}^{(2)}(\Omega, \lambda)}{\left(\mathbb{N}_{11}^{(2)}(\Omega, \lambda) \right)^3},$$

where the right-hand side is given by the measurements. For $k \geq 0$, we recursively define

$$\lambda_{k+1} = f(\lambda_k)$$

until the tolerance criterion

$$\left| \frac{\lambda_{k+1} - \lambda_k}{\lambda_k} \right| < 10^{-10}$$

is met.

- **Step 2.** We compute γ , a_0 and a_m for $m \leq \text{Ord}$ by the explicit formula (35) in Theorem 4.4 (b). With these conformal mapping coefficients, we recover the target anomaly Ω by taking the image of

$$\Psi_{\text{Ord}}(w) = w + a_0 + \frac{a_1}{w} + \frac{a_2}{w^2} + \cdots + \frac{a_{\text{Ord}}}{w^{\text{Ord}}}, \quad |w| = \gamma.$$

Then, real and imaginary parts of $\Psi_{\text{Ord}}(w)$ represent the coordinates of the boundary of the inclusion.

6.2 Examples

We show numerical results of four different shapes of the domains. Figure 2 illustrates the shapes. All four domains satisfy the domain assumption in Theorem 4.4 or in Theorem 5.2. Examples in Figure 2 (a, b) have $C^{1,\alpha}$ boundaries, and examples in Figure 2 (c, d) have boundaries that are piecewise smooth Jordan curves without cusps and satisfy the star-shaped condition in Theorem 5.2. We set $\sigma_m = 1$.

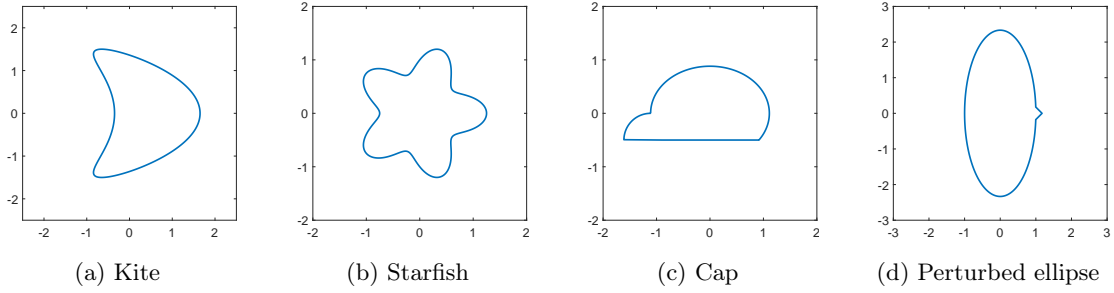


Figure 2: Target geometries of simply connected planar inclusions. The kite- and starfish-shaped domains have $C^{1,\alpha}$ boundaries, and the cap-shaped domain and perturbed ellipse are Lipschitz domains satisfying the star-shaped condition in Theorem 5.2.

To obtain numerical values of the GPTs, we compute the integral definition (3) for the GPTs, where the definition involves a Fredholm second-kind integral equation containing the NP operator, by applying Nyström discretization to this integral equation. See [6, Sections 17.1, 17.3] for numerical codes to compute the GPTs of smooth domains. In our examples with corners, the Nyström discretization is accelerated and stabilized using *recursively compressed inverse preconditioning* (RCIP) [39]. We refer the reader to [24, 40, 41] for computational examples of this procedure.

Example 1 (Kite-shaped domain). First, we consider the kite-shaped inclusion whose shape is portrayed in Figure 2 (a). The boundary curve is parametrized by

$$x(t) = (\cos(t) + 0.65 \cos(2t), 1.5 \sin(t)), \quad t \in [0, 2\pi).$$

Figure 3 presents reconstruction results for the material parameter σ_c (equivalently, $\lambda = \frac{\sigma_c + \sigma_m}{2(\sigma_c - \sigma_m)}$) and shape of the inclusion from the GPTs $\mathbb{N}_{mn}^{(j)}$, $m, n \leq \text{Ord}$, with various Ord. For this and the following examples, the black solid curve indicates the boundary of the target domain, the red dotted curve indicates the recovered boundary, and λ^{rec} denotes the reconstructed value of λ . The imaging accuracy improves as Ord increases. Even with low orders of the GPTs, the location and shape of the target are approximately identified (see Figure 3 (a,b)). The shape recovery scheme precisely produces the shape of the target using higher-order GPTs, as exhibited in Figure 3 (d).

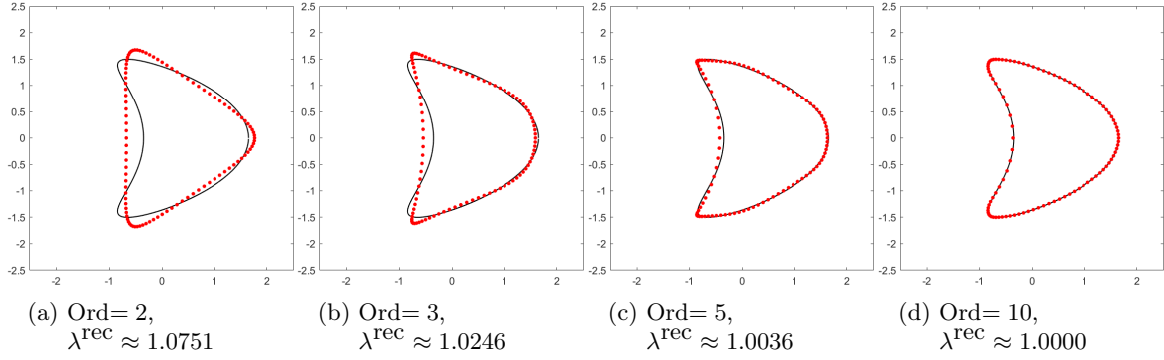


Figure 3: Recovery of the kite-shaped domain with $\sigma_c = 3$ (i.e., $\lambda = 1$). The GPTs $\mathbb{N}_{mn}^{(1)}$ and $\mathbb{N}_{mn}^{(2)}$ are used for $m, n \leq \text{Ord} = 2, 3, 5, 10$. The black solid curve indicates the boundary of the target domain, the red dotted curve indicates the recovered boundary, and λ^{rec} denotes the reconstructed value of λ .

Example 2 (Starfish-shaped domain). In this example, the starfish-shaped domain displayed in Figure 2 (b) is investigated, where the parameterization is given by

$$x(t) = (\cos(t) + 0.25 \cos(5t) \cos(t), \sin(t) + 0.25 \cos(5t) \sin(t)), \quad t \in [0, 2\pi).$$

For the GPTs up to various orders, Figure 4 illustrates reconstruction results for the starfish-shaped domain. The coefficient a_m of this domain decays more slowly than that of the kite-shaped domain in Example 1. To approximate the boundary of the starfish-shaped domain to a high level of accuracy, one needs the GPTs of higher orders than in Example 1. Interestingly, it turns out that, in comparison to the convex parts, recovering the concave part of the boundary is more difficult.

We treat two objects containing corners on their boundary in Example 3 and Example 4.

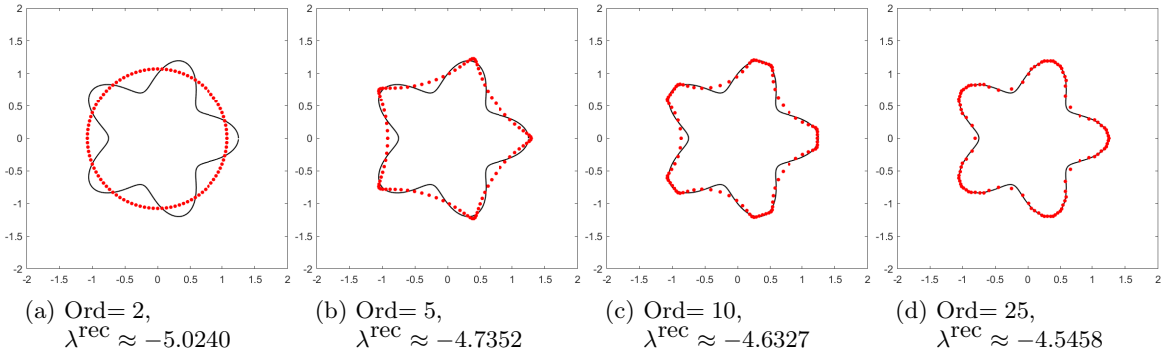


Figure 4: Recovery of the starfish-shape domain with $\sigma = 0.8$ (i.e., $\lambda = -4.5$) from the GPTs of orders up to $\text{Ord} = 2, 5, 10, 25$. The coefficient a_m of this domain decays in m more slowly than that of the kite-shaped domain in Example 1. To accurately retrieve the boundary of the domain, one needs the GPTs of higher orders than for the kite-shaped example.

Example 3 (Cap-shaped domain). We consider the cap-shaped domain in Figure 2(c), which is generated by the boundary parameterization

$$x(t) = \begin{cases} \left(-\frac{1}{2} \sin(4\pi ct) - \frac{\sqrt{2}\pi}{4}, -\frac{1}{2} + \frac{1}{2} \cos(4\pi ct) \right), & t \in [0, t_1], \\ \left(2\pi c(t - t_2) - \sqrt{2} \arcsin\left(\frac{\sqrt{2}}{2} \cos(2\pi a)\right), -\frac{1}{2} \right), & t \in [t_1, t_2], \\ \left(-\sqrt{2} \arcsin\left(\frac{\sqrt{2}}{2} \cos(2\pi c(t - t_2) + 2\pi a)\right), \right. \\ \quad \left. - \operatorname{arcsinh}(\sin(2\pi c(t - t_2) + 2\pi a)) \right), & t \in [t_2, 1], \end{cases}$$

where

$$a = \frac{1}{2} - \frac{1}{2\pi} \arcsin\left(\sinh\left(\frac{1}{2}\right)\right), \quad b = a - \frac{1}{4\pi} - \frac{\sqrt{2}}{8} + \frac{\sqrt{2}}{2\pi} \arcsin\left(\frac{\sqrt{2}}{2} \cos(2\pi a)\right), \quad c = \frac{9}{8} - b, \\ t_1 = \frac{1}{8c} \approx 0.1122, \quad t_2 = t_1 + \left(\frac{a-b}{c}\right) \approx 0.4731.$$

Figure 5 indicates that we can retrieve the conductivity σ_c (or, λ) and shape of an inclusion even when the inclusion has corners on its boundary. As in Example 2, it is more difficult to perfectly recover the concave part of the boundary than the convex part via the proposed method.

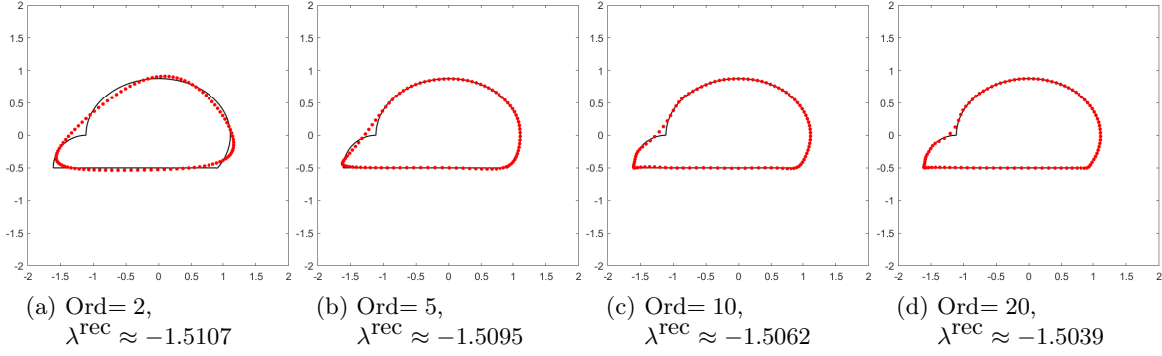


Figure 5: Recovery of the cap-shaped domain with $\sigma = 0.5$ (i.e., $\lambda = -1.5$) from the GPTs of orders up to Ord = 2, 5, 10, 20. The proposed reconstruction scheme works well for this inclusion with corners.

Example 4 (Perturbed ellipse). We consider the perturbed ellipse in Figure 2 (d), which has a tiny corner on its boundary and is generated by the following parameterization

$$x(t) = \begin{cases} \left(\frac{a \cos(t_0) - c_0}{t_0} t + c_0, \frac{b \sin(t_0)}{t_0} t \right), & t \in [0, t_0), \\ (a \cos(t), b \sin(t)), & t \in [t_0, 2\pi - t_0), \\ \left(\frac{a \cos(2\pi - t_0) - c_0}{t_0} (2\pi - t) + c_0, \frac{b \sin(2\pi - t_0)}{t_0} (2\pi - t) \right), & t \in [2\pi - t_0, 2\pi), \end{cases}$$

where

$$a = 1, \quad b = \frac{7}{3}, \quad t_0 = \sin^{-1} \left(\frac{1}{4b\sqrt{2}} \right) \approx 0.0758, \quad c_0 = \sqrt{1 - \frac{1}{32b^2}} + \frac{1}{4\sqrt{2}} \approx 1.1739.$$

Figure 6 displays the reconstruction results with magnified images near the tiny corner. As shown in Figure 6 (d), the small corner can be recovered by the proposed method with high-order GPTs. We note that the corner is smoothened when Ord is not large enough; see Figure 6 (a–c).

7 Conclusion

We developed an analytical method of recovering a planar conductivity inclusion from exterior measurements, where the inclusion is assumed to be a simply connected domain and to be isotropic and homogeneous with arbitrary constant conductivity. Based on the concept of the FPTs, we established matrix factorizations for the GPTs that hold for an inclusion with arbitrary constant conductivity, where the inclusion is either a smooth domain or a star-shaped Lipschitz domain. The matrix factorizations lead us to an inversion formula for a conductivity inclusion. It would be of interest if the proposed inversion scheme—Theorems 4.4 and 5.2—could be extended to a general Lipschitz inclusion not assuming the star-shaped condition. We expect this generalization to be possible considering the shape monotonicity of the GPTs and the smooth approximation for a Lipschitz domain.

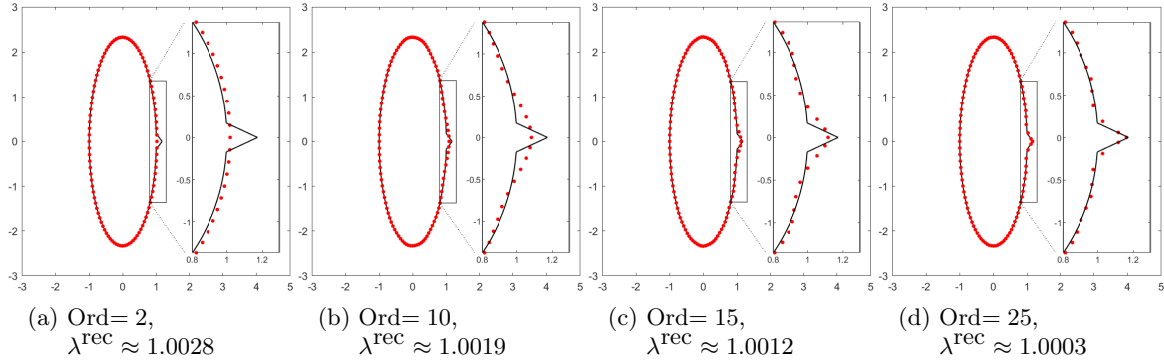


Figure 6: Recovery of the perturbed ellipse with $\sigma = 3$ (i.e., $\lambda = 1$) from the GPTs of orders up to Ord = 2, 10, 15, 25. The image in a rectangle near the tiny corner is magnified. The proposed reconstruction scheme recovers the corner with Ord = 25, while the corner is smoothened when Ord is not large enough.

References

- [1] Andy Adler and David Holder. *Electrical Impedance Tomography: Methods, History and Applications, Medical Physics and Biomedical Engineering*. CRC Press, 2 edition, 2021.
- [2] Lars V. Ahlfors. Quasiconformal reflections. *Acta Math.*, 109:291–301, 1963.
- [3] G. Alessandrini. Singular solutions of elliptic equations and the determination of conductivity by boundary measurements. *J. Differ. Equ.*, 84(2):252–272, 1990.
- [4] H. Ammari, T. Boulier, J. Garnier, W. Jing, H. Kang, and H. Wang. Target identification using dictionary matching of generalized polarization tensors. *Found. Comput. Math.*, 14(1):27–62, 2014.
- [5] H. Ammari, D. Choi, and S. Yu. A mathematical and numerical framework for near-field optics. *Proc. Roy. Soc. A.*, 474(2217), 2018.
- [6] H. Ammari, J. Garnier, W. Jing, H. Kang, M. Lim, K. Sølna, and H. Wang. *Mathematical and statistical methods for multistatic imaging*, volume 2098 of *Lecture Notes in Mathematics*. Springer, Cham, 2013.
- [7] H. Ammari, J. Garnier, H. Kang, M. Lim, and S. Yu. Generalized polarization tensors for shape description. *Numer. Math.*, 126(2):199–224, 2014.
- [8] H. Ammari and H. Kang. Properties of the Generalized Polarization Tensors. *Multiscale Model. Simul.*, 1(2):335–348, 2003.
- [9] H. Ammari and H. Kang. *Polarization and moment tensors*, volume 162 of *Applied Mathematical Sciences*. Springer, New York, 2007. With applications to inverse problems and effective medium theory.
- [10] H. Ammari, H. Kang, and M. Lim. Polarization tensors and their applications. *J. Phys. Conf. Ser.*, 12(1):13–22, 2005.

- [11] H. Ammari, H. Kang, M. Lim, and H. Zribi. Conductivity interface problems. Part I: Small perturbations of an interface. *Trans. Am. Math. Soc.*, 362(5):2435–2449, 2010.
- [12] H. Ammari, H. Kang, M. Lim, and H. Zribi. The generalized polarization tensors for resolved imaging. Part I: Shape reconstruction of a conductivity inclusion. *Math. Comput.*, 81(277):367–386, 2012.
- [13] H. Ammari, M. Putinar, A. Steenkamp, and F. Triki. Identification of an algebraic domain in two dimensions from a finite number of its generalized polarization tensors. *Math. Ann.*, 375(3-4):1337–1354, 2019.
- [14] Habib Ammari, Thomas Boulier, Josselin Garnier, Hyeonbae Kang, and Han Wang. Tracking of a mobile target using generalized polarization tensors. *SIAM Journal on Imaging Sciences*, 6(3):1477–1498, 2013.
- [15] Habib Ammari, Mihai Putinar, Andries Steenkamp, and Faouzi Triki. Reconstruction of domains with algebraic boundaries from generalized polarization tensors. *SIAM Journal on Imaging Sciences*, 12(4):2097–2118, 2019.
- [16] Lorenzo Baldassari and Andrea Scapin. Multi-scale classification for electrosensing. *SIAM Journal on Imaging Sciences*, 14(1):26–57, 2021.
- [17] Liliana Borcea. Electrical impedance tomography. *Inverse Problems*, 18(6):R99–R136, 2002.
- [18] R. Brown and G. Uhlmann. Uniqueness in the inverse conductivity problem for nonsmooth conductivities in two dimensions. *Commun. Partial Differ. Equ.*, 22(5-6):1009–1027, 1997.
- [19] A. Calderón. On an inverse boundary value problem. In *Seminar on Numerical Analysis and its Applications to Continuum Physics (Rio de Janeiro, 1980)*, pages 65–73. Soc. Brasil. Mat., Rio de Janeiro, 1980.
- [20] J. R. Cannon. Determination of the unknown coefficient $k(u)$ in the equation $\nabla \cdot k(u) \nabla u = 0$ from overspecified boundary data. *J. Math. Anal. Appl.*, 18:112–114, 1967.
- [21] C. Carathéodory. Über die gegenseitige Beziehung der Ränder bei der konformen Abbildung des Inneren einer Jordanschen Kurve auf einen Kreis. *Math. Ann.*, 73(2):305–320, 1913.
- [22] P. Caro and K. Rogers. Global uniqueness for the Calderón problem with Lipschitz conductivities. *Forum Math. Pi*, 4:e2, 28, 2016.
- [23] E. Cherkaev, M. Kim, and M. Lim. Geometric series expansion of the Neumann–Poincaré operator: Application to composite materials. *Eur. J. Appl. Math.*, pages 1–26, 2021.
- [24] D. Choi, J. Helsing, and M. Lim. Corner effects on the perturbation of an electric potential. *SIAM J. Appl. Math.*, 78(3):1577–1601, 2018.
- [25] D. Choi, J. Kim, and M. Lim. Geometric multipole expansion and its application to neutral inclusions of general shape. *arXiv:1808.02446*, 2018.
- [26] D. Choi, J. Kim, and M. Lim. Analytical shape recovery of a conductivity inclusion based on Faber polynomials. *Math. Ann.*, 381(3-4):1837–1867, 2021.

- [27] C. K. Chui, J. Stöckler, and J. D. Ward. A Faber series approach to cardinal interpolation. *Math. Comput.*, 58(197):255–273, 1992.
- [28] J. H. Curtiss. Harmonic interpolation in Fejér points with the Faber polynomials as a basis. *Math. Z.*, 86:75–92, 1964.
- [29] J. H. Curtiss. Solutions of the Dirichlet problem in the plane by approximation with Faber polynomials. *SIAM J. Numer. Anal.*, 3:204–228, 1966.
- [30] V Druskin. The unique solution of the inverse problem of electrical surveying and electrical well-logging for piecewise-continuous conductivity. *Izvestiya, Earth Physics (in Russian)*, 18(1):51–53, 1982.
- [31] Vladimir Druskin. On the uniqueness of inverse problems from incomplete boundary data. *SIAM J. Appl. Math.*, 58(5):1591–1603, 1998.
- [32] P. L. Duren. *Univalent functions*, volume 259 of *Grundlehren der Mathematischen Wissenschaften*. Springer-Verlag, New York, 1983.
- [33] S. W. Ellacott. Computation of Faber series with application to numerical polynomial approximation in the complex plane. *Math. Comput.*, 40(162):575–587, 1983.
- [34] L. Escauriaza, E. B. Fabes, and G. Verchota. On a regularity theorem for weak solutions to transmission problems with internal Lipschitz boundaries. *Proc. Am. Math. Soc.*, 115(4):1069–1076, 1992.
- [35] G. Faber. Über polynomische Entwicklungen. *Math. Ann.*, 57(3):389–408, 1903.
- [36] T. Feng, H. Kang, and H. Lee. Construction of GPT-vanishing structures using shape derivative. *J. Comput. Math.*, 35(5):569–585, 2017.
- [37] C.F. Gao and N. Noda. Faber series method for two-dimensional problems of an arbitrarily shaped inclusion in piezoelectric materials. *Acta Mech.*, 171(1):1–13, 2004.
- [38] A. Greenleaf, M. Lassas, and G. Uhlmann. The Calderón problem for conormal potentials. I. Global uniqueness and reconstruction. *Commun. Pure Appl. Math.*, 56(3):328–352, 2003.
- [39] J. Helsing. Solving integral equations on piecewise smooth boundaries using the RCIP method: a tutorial. *Abstr. Appl. Anal.*, pages Art. ID 938167, 20 pages, 2013.
- [40] J. Helsing and S. Jiang. Solving fredholm second-kind integral equations with singular right-hand sides on non-smooth boundaries. *J. Comput. Phys.*, 448:110714, 2022.
- [41] J. Helsing, H. Kang, and M. Lim. Classification of spectra of the Neumann-Poincaré operator on planar domains with corners by resonance. *Ann. Inst. Henri Poincaré (C) Anal. Non Linéaire*, 34(4):991–1011, 2017.
- [42] J. Helsing and R. Ojala. Corner singularities for elliptic problems: integral equations, graded meshes, quadrature, and compressed inverse preconditioning. *J. Comput. Phys.*, 227(20):8820–8840, 2008.

- [43] D. Isaacson, J.L. Mueller, J.C. Newell, and S. Siltanen. Reconstructions of chest phantoms by the D-bar method for electrical impedance tomography. *IEEE Trans. Med. Imaging*, 23(7):821–828, 2004.
- [44] Y. Jung and M. Lim. A decay estimate for the eigenvalues of the Neumann-Poincaré operator using the grunsky coefficients. *Proc. Am. Math. Soc.*, 148(2):591–600, 2020.
- [45] Y. Jung and M. Lim. Series Expansions of the Layer Potential Operators Using the Faber Polynomials and Their Applications to the Transmission Problem. *SIAM J. Math. Anal.*, 53(2):1630–1669, 2021.
- [46] H. Kang, H. Lee, and M. Lim. Construction of conformal mappings by generalized polarization tensors. *Math. Methods Appl. Sci.*, 38(9):1847–1854, 2015.
- [47] O. D. Kellogg. *Foundations of Potential Theory*, volume 31 of *Die Grundlehren der Mathematischen Wissenschaften*. Springer-Verlag Berlin Heidelberg, 1929.
- [48] K. Knudsen and A. Tamasan. Reconstruction of less regular conductivities in the plane. *Commun. Partial Differ. Equ.*, 29(3-4):361–381, 2004.
- [49] R. Kohn and M. Vogelius. Determining conductivity by boundary measurements. *Commun. Pure Appl. Math.*, 37(3):289–298, 1984.
- [50] R. Kohn and M. Vogelius. Determining conductivity by boundary measurements. II. Interior results. *Commun. Pure Appl. Math.*, 38(5):643–667, 1985.
- [51] J. C Luo and C. F. Gao. Faber series method for plane problems of an arbitrarily shaped inclusion. *Acta Mech.*, 208(3):133, 2009.
- [52] A. I. Nachman. Global Uniqueness for a Two-Dimensional Inverse Boundary Value Problem. *Ann. Math.*, 143(1):71–96, 1996.
- [53] R. G. Novikov. Multidimensional inverse spectral problem for the equation $-\Delta\psi + (v(x) - Eu(x))\psi = 0$. *Funct. Anal. Appl.*, 22(4):263–272, 1988.
- [54] R. G. Novikov. An effectivization of the global reconstruction in the Gel’fand-Calderón inverse problem in three dimensions. In *Imaging microstructures*, volume 494 of *Contemp. Math.*, pages 161–184. Amer. Math. Soc., Providence, RI, 2009.
- [55] L. Päiväranta, A. Panchenko, and G. Uhlmann. Complex geometrical optics solutions for Lipschitz conductivities. *Rev. Mat. Iberoam.*, 19(1):57–72, 2003.
- [56] G. Pólya and G. Szegő. *Isoperimetric Inequalities in Mathematical Physics*. Annals of Mathematics Studies, no. 27. Princeton University Press, Princeton, N. J., 1951.
- [57] C. Pommerenke. *Univalent functions*. Vandenhoeck & Ruprecht, Göttingen, 1975.
- [58] C. Pommerenke. *Boundary behaviour of conformal maps*, volume 299 of *Grundlehren der Mathematischen Wissenschaften*. Springer-Verlag, Berlin, 1992.
- [59] J. Sylvester and G. Uhlmann. A global uniqueness theorem for an inverse boundary value problem. *Ann. of Math. (2)*, 125(1):153–169, 1987.

- [60] A. N. Tikhonov. On the uniqueness of the solution of the problem of electric prospecting. *Dokl. Akad. Nauk SSSR (in Russian)*, 69(6):797–800, 1949.
- [61] A. N. Tikhonov. On determining electrical characteristics of the deep layers of the Earth’s crust. *Dokl. Akad. Nauk SSSR*, 73(2):295–297, 1950.
- [62] G. Uhlmann. Electrical impedance tomography and Calderón’s problem. *Inverse Problems*, 25(12):123011, 39, 2009.
- [63] G. Verchota. Layer potentials and regularity for the Dirichlet problem for Laplace’s equation in Lipschitz domains. *J. Funct. Anal.*, 59(3):572–611, 1984.
- [64] M. Wala and A. Klöckner. Conformal mapping via a density correspondence for the double-layer potential. *SIAM J. Sci. Comput.*, 40(6):A3715–A3732, 2018.